Extending the enzymatic toolbox for heparosan polymerization, depolymerization, and detection

Malgorzata Sulewska, Monika Berger, Manuela Damerow, David Schwarzer, Falk F R Buettner, Andrea Bethe, Manuel H Taft, Hans Bakker, Martina Mühlenhoff, Rita Gerardy-Schahn, et al.

▶ **To cite this version:**

Malgorzata Sulewska, Monika Berger, Manuela Damerow, David Schwarzer, Falk F R Buettner, et al.. Extending the enzymatic toolbox for heparosan polymerization, depolymerization, and detection. Carbohydrate Polymers, 2023, 319, pp.121182. ⟨10.1016/j.carbpol.2023.121182⟩. ⟨hal-04882031⟩

HAL Id: hal-04882031

https://hal.science/hal-04882031v1

Submitted on 13 Jan 2025

HAL is a multi-disciplinary open access archive for the deposit and dissemination of scientific research documents, whether they are published or not. The documents may come from teaching and research institutions in France or abroad, or from public or private research centers.

L'archive ouverte pluridisciplinaire **HAL**, est destinée au dépôt et à la diffusion de documents scientifiques de niveau recherche, publiés ou non, émanant des établissements d'enseignement et de recherche français ou étrangers, des laboratoires publics ou privés.

HAL Authorization

Extending the enzymatic toolbox for heparosan polymerization, depolymerization, and detection

Małgorzata Sulewska [a,b], Monika Berger [a], Manuela Damerow [a], David Schwarzer [a], Falk F.R. Buettner [a], Andrea Bethe [a], Manuel H. Taft [c], Hans Bakker [a], Martina Mühlenhoff [a], Rita Gerardy-Schahn [a], Bernard Priem [b], Timm Fiebig [a,*]

[a] *Institute of Clinical Biochemistry, Hannover Medical School, Hannover, Germany*
[b] *Centre de Recherche sur les Macromolécules Végétales, Groupe Chimie et Biotechnologie des Oligosaccharides, 601 rue de la Chimie, BP 53X, 38041 Grenoble, Cedex 09, France*
[c] *Institute for Biophysical Chemistry, Hannover Medical School, Hannover, Germany*

ARTICLE INFO

Keywords:
Heparosan
Lyase
Glycosaminoglycans
Enzymatic synthesis
Bacteriophage
Tailspike protein

ABSTRACT

Heparosan is an acidic polysaccharide expressed as a capsule polymer by pathogenic and commensal bacteria, e.g. by *E. coli* K5. As a precursor in the biosynthesis of heparan sulfate and heparin, heparosan has a high biocompatibility and is thus of interest for pharmaceutical applications. However, due to its low immunogenicity, developing antibodies against heparosan and detecting the polymer in biological samples has been challenging.

In this study, we exploited the enzyme repertoire of *E. coli* K5 and the *E. coli* K5-specific bacteriophage ΦK5B for the controlled synthesis and depolymerization of heparosan. A fluorescently labeled heparosan nonamer was used as a priming acceptor to study the elongation mechanism of the *E. coli* K5 heparosan polymerases KfiA and KfiC. We could demonstrate that the enzymes act in a distributive manner, producing labeled heparosan of low dispersity. The enzymatically synthesized heparosan was a useful tool to identify the tailspike protein KflB of ΦK5B as heparosan lyase and to characterize its endolytic depolymerization mechanism. Most importantly, using site-directed mutagenesis and rational construct design, we generated an inactive version of KflB for the detection of heparosan in ELISA-based assays, on blots, and on bacterial and mammalian cells.

1. Introduction

Heparosan is a natural, acidic polysaccharide belonging to the glycosaminoglycan (GAG) family. Its dimeric repeating unit consists of [-4-*N*-acetylglucosamine(GlcNAc)-α1,4-glucuronic acid(GlcA)-β1-] (DeAngelis, 2015). Heparosan is expressed by pathogenic bacteria such as *Escherichia coli* K5 and *Pasteurella multocida* and by non-pathogenic bacteria like *E. coli* Nissle 1917 (Cress et al., 2014). As a natural precursor for synthesizing heparin and heparan sulfate, heparosan is recognized as "self", which facilitates evasion of the host immune response (Cress et al., 2014). Due to its stability in extracellular spaces (Jing et al., 2017), its high biocompatibility, and its lack of immunogenicity, heparosan could be used as drug delivery system (Lane et al., 2017). Consequently, developing a toolbox for the synthesis, engineering and detection of heparosan has received much attention (Zhang et al., 2019). So far, this toolbox contains, e.g., engineered bacteria for the production of functionalized heparosan (Leroux & Priem, 2016; Priem et al., 2017), bacterial polymerases for the enzymatic synthesis of heparosan (He et al., 2022; Na et al., 2020; Otto et al., 2012; Sismey-Ragatz et al., 2007), heparosan lyases (Clarke et al., 2000; Thompson et al., 2010), other means to disassemble heparosan (Higashi et al., 2011), as well as RNA-based reagents for the detection of the polymer (Kizer et al., 2018). Especially due to the lack of immunogenicity, producing antibodies against heparosan is difficult (DeAngelis, 2015; Kizer et al., 2018). Thus, it is of importance to develop specific, robust and easy-to-use reagents for the detection of heparosan in e.g. biological

* Corresponding author.
E-mail addresses: Sulewska.Malgorzata@mh-hannover.de (M. Sulewska), Berger.Monika@mh-hannover.de (M. Berger), Publishing@davidschwarzer.de (D. Schwarzer), Buettner.Falk@mh-hannover.de (F.F.R. Buettner), Bethe.Andrea@mh-hannover.de (A. Bethe), Taft.Manuel@mh-hannover.de (M.H. Taft), Bakker.Hans@mh-hannover.de (H. Bakker), Muehlenhoff.Martina@mh-hannover.de (M. Mühlenhoff), Gerardy-Schahn.Rita@mh-hannover.de (R. Gerardy-Schahn), bernard.priem@cermav.cnrs.fr (B. Priem), Fiebig.Timm@mh-hannover.de (T. Fiebig).

samples.

E. coli K5 contains a heparosan synthase consisting of two, separately expressed GT-A fold enzymes named KfiA and KfiC, which are part of a group 2 capsule expression system (Sande & Whitfield, 2021; Sugiura et al., 2010). They are co-expressed with (i) KfiB, which is speculated to promote membrane localization and is supposed to have a scaffolding function (Cress et al., 2014; Hodson et al., 2000), and (ii) KfiD, a UDP-glucose dehydrogenase responsible for providing UDP-GlcA, the substrate of KfiC (Sieberth et al., 1995). Interestingly, KfiC can only transfer GlcA to the non-reducing end of the nascent chain if KfiA is present, whereas KfiA can catalyse single GlcNAc transfers even in the absence of KfiC (Sugiura et al., 2010). However, information about the elongation mechanism utilized by KfiC and KfiA (from here on referred to as KfiCA if used together) is missing. Thus, one aim of this study was to elucidate the mechanism of elongation and evaluate the suitability of KfiCA for the in vitro synthesis of heparosan of different sizes.

Available means for the depolymerisation of heparosan include the phage tailspike protein (TSP) KflA (Clarke et al., 2000) and the putative pro-phage derived eliminase ElmA (Legoux et al., 1996). Both enzymes have been studied biochemically (Schwarzer et al., 2007; Thompson et al., 2010), and a crystal structure shows that KflA adopts a trimeric single-stranded β-helix fold (Thompson et al., 2010). Some TSPs, like the polysialic acid-degrading endosialidase of phage ΦK1F (endoNF), have different polymer binding sites distant from the catalytic center (Stummeyer et al., 2005). It has been shown that the catalytic center can be deactivated without destroying the polymer binding site, which led to the development of a detection agent for polysialic acid (Stummeyer et al., 2005). Since the structure of KflA was obtained without polymer, it is unknown if bacteriophage-derived heparosan lyases exploit the same multivalent binding mode and if they can be transformed into a detection agent for heparosan. Bacterial heparinases are useful tools for the structural analysis of heparin and heparan sulfate (Boyce & Walsh, 2022) and can contain extended oligosaccharide binding sites (Han et al., 2009). However, these enzymes are structurally distinct from KflA (Thompson et al., 2010) and, to the best of our knowledge, have not been transformed into detection agents yet.

This study is based on the hypothesis that *E. coli* K5-based polymerases and lyases can broaden the toolbox for heparosan synthesis, depolymerization, and detection. We generated a fluorescently labeled oligosaccharide to characterize the elongation mechanism of KfiA and KfiC, demonstrating that these enzymes can be exploited to synthesize fluorescently labeled heparosan of different sizes. We further show that the tailspike protein KflB from the as yet undescribed *E. coli* K5-specific phage ΦK5B has heparosan lyase activity. We present an extensive biochemical characterization of KflB using natural and fluorescently labeled heparosan as a substrate. Finally, we demonstrate that the enzyme can be engineered to become a detection agent for heparosan.

2. Materials and methods

2.1. Materials

Enzymes were purchased from Thermo Fisher Scientific and New England Biolabs GmbH. Recombinant DNA was isolated with QiAprep Spin Miniprep Kit (Qiagen Inc.). An overview of bacterial strains used in this study is given in Supplementary Table S1. The antibiotics used for bacterial cultures were: ampicillin (100 μg/mL), carbenicillin (50 μg/mL), chloramphenicol (20 μg/mL), kanamycin (50 μg/mL), and tetracycline (15 μg/mL). The *E. coli* K5-specific ΦK5B (isolated from sewer) was kindly provided by Prof. Dr. Dieter Bitter-Suermann (Hannover Medical School) and sequenced at the Institute of Clinical Biochemistry. The sequence for KflB is provided in Supplementary Fig. S4. All primers used for cloning are listed in Supplementary Tables S2, S3.

The following commercially available GAGs were used in this study: Dermatan sulfate (Iduron, GAG-DS01, 41.4 kDa), chondroitin sulfate (C6737, Sigma), heparan sulfate (Iduron, GAG-HS01 (mixture of 9 and 35 kDa, 80 % sulfation), GAG-HS I (40 kDa, 75 % sulfation, used for microscale thermophoresis)), heparin (Sigma/Merck, H3393), hyaluronic acid/hyaluronan (Dextra, PS116, 1.5–2.2 MDa), hyaluronic acid/hyaluronan standards (Echelon Biosci, HYA-LOLAD, HYA-0025 (25 kDa), HYA-0075 (75 kDa), HYA-0200 (200 kDa)).

2.2. HPLC-based anion-exchange chromatography (HPLC-AEC)

HPLC-AEC was performed on a Prominence UFLC-XR system (Shimadzu) using a CarboPac PA-100 column (Dionex™; 2 × 250 mm). Separation of the analytes was performed at 50 °C at a flow rate of 0.6 mL/min using ultrapure water as mobile phase A and 1 M NaCl as mobile phase B. Unlabeled heparosan with non-reducing end Δ4,5 GlcA was detected at a wavelength between 232 and 250 nm as indicated. Heparosan labeled with 2AB was detected by fluorescence detection (Exc. $\lambda = 330$ nm, Emi. $\lambda = 420$ nm). The details of the elution conditions are described for each relevant experiment. All the samples from bacterial lysates were filtrated using Ultrafree™-centrifugal filter units (Millipore; 0.22 μm; 16,000 ×*g*, 5 min) prior to the HPLC-AEC analysis.

2.3. Cloning

2.3.1. Engineered heparosan synthases

To generate the pBAD33-based plasmid expressing untagged KfiCA under one promoter, first *kfiC* from pEX-A258-*kfiCs* (Eurofins Genomics, see Supplementary Fig. S2), and then *kfiA* from pBS-*kfiA* (Priem et al., 2017) were inserted into pBAD33 via *Kpn*I/*Hin*dIII and *Xba*I/*Pst*I, respectively, yielding pBAD33-*kfiCA* (6225, see Supplementary Table S2). To obtain pBAD33-*kfiCAB* (5744), *kfiB* was first cloned from pBBR-glcAT-*kfiDB* (Priem et al., 2017) via *Spe*I/*Sac*I into pBBR-MCS3 (Kovach et al., 1995), yielding pBBR1-MCS3-*kfiB*. Subsequently, *kfiB* was cloned from pBBR1-MCS3-*kfiB* via *Xho*I/*Pvu*I into pBAD33-*kfiCA*, yielding pBAD33-*kfiCAB* (5744). A plasmid encoding KfiD (pBBR1-MCS3-kfiD) was obtained from (Leroux & Priem, 2016) and labeled 5691.

Tagged KfiA and KfiB intended for purifications were generated as follows: *kfiA* and *kfiB* were amplified by PCR from pBS-*kfiA* (Priem et al., 2017) and pBBR1-MCS3-kfiB using primers MS05, MS02 and MS10, MS11 (Supplementary Tables S2 and S3), respectively. The obtained PCR products coding for KfiA and KfiB were cloned into modified versions of pMBP-S3N10-*csxA*-His_6 (tac) (Fiebig et al., 2014) via restriction-free cloning (Bond & Naus, 2012). In the resulting constructs pMal-c-His_6-*kfiA* (5644) and pMal-c-MBP-S3N10-preScission-*kfiB*-His_6 (5668), KfiA is N-terminally fused to a His_6 tag, and KfiB is N-terminally linked via a PreScission cleavage site and an S3N10 linker to a maltose binding protein (MBP), and C-terminally fused to a His_6 tag. For improved solubility, KfiC was fused with trigger factor (TF) to create a construct as previously described (Leroux & Priem, 2016; Sugiura et al., 2010). TF was cloned via *Nde*I/*BamHI* from pBS-His_6-TF (Leroux & Priem, 2016) into pET28a. Subsequently, KfiC from pEX-A258-*kfiCs* (Eurofins Genomics) was cloned via BamHI/HindIII into pET28a-His_6-TF vector, yielding pET28a-His_6-TF-kfiC (5822).

2.3.2. Engineered K5 lyase B and its mutants

The gene encoding KflB was amplified using the primers MM315 and MM317 (Supplementary Table S2). The amplicon was inserted via *BamHI*/*XhoI* into pStrep-D245*EndoNF*-His_6 (Schwarzer et al., 2009), replacing D245EndoNF. The start codon (ATG) at nucleotide position 1–3 of *kflB* was removed via restriction-free cloning (Bond & Naus, 2012) with the primers MS49 and MS50 (Supplementary Table S2) generating pStrep-*kflB*-His_6 (6118). pStrep-*kflB*-Y229A-His_6 (6119) and pStrep-*kflB*-S505A-His_6 (6122) were generated using site-directed mutagenesis with primers DS210, DS211 and MR01, MR02, respectively, and 6118 as a template (Supplementary Tables S2 and S3). Single alanine substitutions in 6112, 6113, and 6114 (F202, E206, K208A) were introduced according to Liu et al. (Liu & Naismith, 2008) using the

primers indicated in Supplementary Tables S2 and S3 and Strep-*kflB*-His_6 (6118) as a DNA template. Additional mutations were generated using the single mutants as DNA template. The sequence encoding eGFP-GS24 was amplified from pET22b-Strep II-*eGFP*-GS24-*ΔN-endoNF* (Kiermaier et al., 2016) with primers MS73 and MS74 (Supplementary Table S3) and cloned into 6168 using the restriction-free cloning protocol (Bond & Naus, 2012) generating 6338. The ALFA-tag (Götzke et al., 2019) was introduced by restriction-free cloning into Strep-*kflB*-E206A, K208A-His_6 using the primers indicated in Supplementary Table S2. All plasmids were propagated in *E. coli* XL1 Blue, and the sequence identity of the coding sequences was confirmed by Sanger sequencing (Eurofins Genomics).

2.4. Heparosan preparation and characterization

2.4.1. Heparosan production

Heparosan was produced using *E. coli* BJ transformed with plasmids expressing KfiCAB (5744) and KfiD (5691) (see Supplementary Table S2) as previously described by Barreteau et al. (2012) with the following changes: The fed-batch phase started with the addition of the continuous feeding solution (50 % glycerol and 0.5 % L-arabinose). After 30 min, isopropyl 1-thio-β-D-galactopyranoside (IPTG) was added at a final concentration of 0.2 mM.

2.4.2. Heparosan fractionation

Heparosan (100 mg/mL) was dissolved in water and loaded on a HiTrap Q HP column (Cytiva) preequilibrated with water. Heparosan was eluted with 1 M NaCl using a linear gradient from 0 to 480 mM NaCl over 40 column volumes. Fractions were collected and analyzed on 15 % PA gel stained with Alcian blue/silver. Fractions, as indicated in Supplementary Fig. S6a, were pooled, lyophilized, dialyzed (Zellu Trans, Roth, 10 kDa MWCO) against water, and lyophilized again.

2.4.3. Heparosan characterization by HPAEC-PAD

HPAEC-PAD was performed on an ICS 5000 system (Dionex, Thermo Fisher Scientific) equipped with a CarboPac PA200 column (Thermo Fisher Scientific). Samples were separated at 30 °C with a flow rate of 0.5 mL/min using mobile phases M1 (100 mM NaOH), M2 (100 mM NaOH, 1 M NaOAc), M3 (H_2O) and M4 (500 mM NaOH) and the following gradient: Step 1, 0–5 min, 24 % M2, 76 % M1; Step 2, 5–45 min, 24–64 % M2, 76–36 % M1; Step 3, 45–60 min, 64–79 % M2, 36–21 % M1; Step 4, 60–102 min 79–100 % M2, 21–0 % M1. The column was washed for 5 min with 100 % M4 and equilibrated for 10 min with 24 % M2 and 76 % M1.

2.5. Preparation of the fluorescently labeled K5 oligosaccharide acceptor

2.5.1. Production of intracellular K5-derived oligosaccharides

Generation, extraction, and purification of heparosan oligosaccharides were performed according to a previously published protocol (Barreteau et al., 2012) with the following changes. The acidic supernatant was neutralized with the Amberlite FPA66 anion-exchange free base (Sigma-Aldrich), and the centrifugation step (30 min, 7000 rpm) was repeated to remove the resin. Generated oligosaccharides were detected by a thin layer chromatography-based protocol developed by Zhang et al. (2007). In the final step, oligomers were separated by size exclusion chromatography with a Hiload Superdex S30x3 column (26 × 600 mm, GE Healthcare) with 0.1 M ammonium carbonate at a flow rate of 1.2 mL/min as a mobile phase. The appropriate fractions of oligomers were pooled, concentrated in vacuo, and lyophilized, yielding heparosan oligomers with a degree of polymerization (DP) from 2 to 12.

2.5.2. Fluorescent labeling of the K5 oligosaccharide acceptor

Heparosan decamer **1** underwent treatment with mercury (II) acetate as described by Ludwigs et al. (1987). The solution was passed through a column filled with Dowex 50 W-X8 (H^+ form; Sigma-Aldrich). The filtrate was lyophilized to give a white, solid product **2**. Compound **2** was labeled using 2-aminobenzamide (2AB) according to a published protocol (France et al., 2000) with the following changes: the crude product was precipitated with cold acetone and centrifuged (4 °C, 20 min, 4000*g*). The supernatant was discarded, and residues were neutralized with 1 M HCl for 1 h at room temperature under stirring. The reaction mixture was concentrated in vacuo. The crude product was purified by silica chromatography (acetonitrile/water = 9:1 ➔ 0:1) to give a yellowish solid **3**.

2.6. Protein expression and purification

2.6.1. Expression and purification

Overnight bacterial cultures (*E. coli* M15[pREP4] for 5644, 5668; BL21(DE3) for 5822, and all KflB constructs) were grown in PowerBroth (Athena Enzyme System) supplemented with carbenicillin (pKfiA, pKfiB, and all KflB constructs) or kanamycin (pKfiC) at 37 °C until an optical density (OD_{600}) of ~1.0 was reached. After cooling at 4 °C for app. 30 min, expression of pKfiCAB and KflB constructs was induced by 0.1 mM IPTG and 0.5 mM IPTG, respectively. Bacteria were harvested after overnight incubation at 15 °C. Cells expressing pKfiCAB were lysed by sonication on ice in buffer A (50 mM Tris, pH 8.0, 500 mM NaCl, 10 mM imidazole), while KflB proteins were sonicated on ice in buffer W (100 mM Tris, pH 8.0, 150 mM NaCl, 1 mM EDTA). Both buffers contained EDTA-free protease inhibitors (complete EDTA-free, Roche). The suspension was sonicated (Sonifier 450, Branson) 10–12 times at a 30 % amplitude for 30 s on ice with 30 s cooling on ice in between each sonication step. The resulting lysates were centrifuged for 3 min at 16,000 x *g*. Soluble fractions containing pKfiCAB were loaded on His Trap HP columns (1 mL; GE Healthcare) and gradually eluted with buffer B (50 mM Tris, pH 8.0, 500 mM NaCl, 500 mM imidazole; linear elution with 50–500 mM imidazole over 20 min). Recombinant KflB proteins were purified using StrepTactin columns (IBA) and eluted according to the manufacturer's instructions.

2.6.2. Size-exclusion chromatography (SEC)

Proteins were concentrated by centrifugation using centrifugal devices (Amicone, Millipore). The concentrated sample was loaded onto a Superdex 200 HR 10/30 column (Amersham Biosciences). Column equilibration and elution were performed with 10 mM Tris-HCl, pH 8.0, 50 mM NaCl, 1 mM DTT at 0.5 mL/min. SEC of Strep-KflB-E206A, K208A intended for fluorescent labeling was performed in phosphate-buffered saline (PBS).

2.7. Elongation of the K5 oligosaccharide acceptor – fluorescent heparosan

Non-tagged KfiCA (6225) were expressed in BL21(DE3) (Supplementary Table S2) and grown in PowerBroth with chloramphenicol selection. The procedure was similar to the expression of tagged proteins, with the following changes: expression was induced at $OD_{600} = 0.5$ with L-arabinose (Roth) at the final concentration of 0.1 %. A 1 mL aliquot of bacterial culture with $OD_{600} = 2.0$ was centrifuged and the obtained pellet was washed four times with buffer C [100 mM Bis-Tris (Sigma), pH 6.5, 5 mM NaCl]. Next, the pellet was resuspended in buffer C containing 0.1 mg/mL lysozyme (Serva) and EDTA-free protease inhibitors (complete EDTA-free, Roche). After 10 min of incubation in the lysis mixture, cells were lysed by three cycles of sonication (Sonorex sonicator, Bandelin, duty cycle: constant; output control: 5; timer: hold) in a cooled sonication bath for 45 s with at least 1 min cooling on ice in between each sonication step. The soluble fraction was used in in vitro assays. To elongate 3 μM of the K5 oligosaccharide acceptor, 80 μL of expressed non-tagged KfiCA or 4 μM of tagged, purified proteins (pKfiC, pKfiA and if indicated pKfiB) were used in a total reaction volume of 1 mL or 100 μL, respectively. The reaction mixture was supplemented with 1 mM uridine diphosphate *N*-acetylglucosamine [UDP-GlcNAc (Sigma-

Aldrich)], uridine diphosphate D-glucuronic acid [UDP-GlcA (Sigma-Aldrich)], 1 mM dithiothreitol [DTT (Sigma)] and 15 % glycerol (Sigma) in a buffer comprising 250 mM Bis-Tris pH 6.5, 25 mM NaCl and 10 mM $MgCl_2$. The reaction was incubated at 37 °C for the indicated time points. Enzymes were inactivated by incubation at 70 °C for 20 min, and the precipitate was removed by centrifugation (16,000 ×*g*, 5 min). The samples (25 µL) were analyzed by HPLC-AEC coupled to fluorescence detection (Exc. λ = 330 nm, Emi. λ = 420 nm). The chromatograms (Fig. 2B, C) were recorded using a −3 curved gradient from 0 to 20 % of mobile phase B (see 2.2) over 5 min, followed by a linear gradient from 20 to 52 % of mobile phase B over 39 min. The gradient was calibrated using Select-HA^{Tm} 25 k, Select-HA^{Tm} 75 k and Select-HA^{Tm} 200 k (tebu-bio GmbH, see 2.1).

2.8. K5 lyase B activity assays

2.8.1. Activity

KflB constructs (0.2–2 µM) were incubated with 2.8–10 µg/µL of heparosan in assay buffer (25 mM Tris-HCl, pH 8.0, 50 mM NaCl) with 1 mM DTT at 37 °C. Samples (18–20 µL) were taken as indicated (Fig. 4B, D) and immersed in liquid nitrogen or incubated at 80 °C for 20 min to stop the reaction. Analysis was carried out using HPLC-AEC coupled to UV detection (λ = 250 nm). Separation was achieved using a 16 % linear gradient of mobile phase B over 7 min, followed by a −1 curved gradient from 16 to 30 % over 30 min, and a +1 curved gradient from 30 to 50 % over 6 min. Moreover, samples were analyzed via Alcian blue/silver staining after PAGE (Fig. 4A, C, Fig. 8).

KflB wt (1 nM) was added to 185 µL of the overnight heparosan synthesis reaction shown in Fig. 2B and described in 2.7, and supplemented with water to a total volume of 200 µL. The reaction mixture was incubated at 37 °C, samples (20 µL) were taken at the indicated time points, incubated at 80 °C for 20 min to stop the reaction, and analyzed via HPLC-AEC coupled to fluorescence detection as described in 2.7.

2.8.2. The minimal length of the KflB substrate

Heparosan oligosaccharides (DP = 4, 6, 8, 10; 10 µg/µL) were incubated at 37 °C overnight in the assay buffer with 1 µM of KflB wt in a total reaction volume of 80 µL. Samples (4–8 µL) were analyzed via HPLC-AEC coupled to UV detection (λ = 232 nm) using a 30 % linear gradient of mobile phase B (from 3 to 14 min).

2.8.3. KflB specificity determination

To determine KflB substrate specificity, 1 mg/mL of a substrate as indicated was incubated with 4.5 µM KflB wt in a total volume of 25 µL at 37 °C. Samples were taken after half an hour, two hours, and overnight incubation. The reactions were stopped by immersion in liquid nitrogen, and polymers were visualized by Alcian blue/silver staining after PAGE.

2.9. Labeling of an inactive KflB

Purified Strep-KflB-E206A, K208A (6168) (73.3 µL, 3.13 nmol, 1 equiv.) in PBS was mixed with IR Dye 800CW NHS Ester (1.1 µL, 9.4 nmol, 3 equiv.; LI-COR Biosciences) in DMF and incubated at 4 °C for 15 h. The non-reacted dye was removed with Zeba™ Dye and Biotin Removal Spin Columns (ThermoFisher Scientific) according to the manufacturer's guidelines. The obtained fluorescently labeled protein is referred to as iKflB IR800.

2.10. Detection of GAGs using iKflB

A sample of an engineered heparosan-producing strain was prepared as described in 2.4. *E. coli* K1, *E. coli* K5, and *E. coli* BJ (selected with tetracycline) (Supplementary Table S1) were cultivated overnight in PowerBroth at 37 °C. Liquid bacterial cultures (OD_{600} = 2.6) were transferred (80 µL, 40 µL and 20 µL) onto a nitrocellulose membrane and air-dried. Subsequently, membranes were incubated in Intercept® (PBS) Blocking Buffer (BB, LI-COR Biosciences) and PBS at a ratio of 1:2 at 4 °C overnight. Heparosan was directly detected using iKflB IR800 [1:3000 in BB:PBS (1:2)]. If Strep-eGFP-GS24-iKflB (6338) [20 µg/mL in BB:PBS (1:2)] was used for detection, additional incubation steps with Avidin [2 µg/mL in BB:PBS (1:2) for 10 min; (Sigma-Aldrich)] and Strep-Tactin IR 800CW (1:2000) were performed. Each incubation was performed at room temperature for 1 h (unless stated otherwise) with orbital shaking at 13 rpm. The membrane was washed four times with 0.1 % Tween® 20 in PBS (PBS-T) after each incubation with detection agents. For visualization, membranes were scanned using an Odyssey® infrared imaging system (LI-COR Biosciences).

For the detection of purified GAGs, 1 µg of commercially available GAGs (see 2.1) as indicated and 0.48–15.4 µg of unfractionated heparosan were spotted onto a nitrocellulose membrane and the membrane was air-dried. Blocking and detection was achieved as described above with the difference that 15 µg/mL (180 nM) of 6338 was used.

For electro-transfer blotting, 5 µg of GAGs were separated using PAGE as previously described (Litschko et al., 2021) and then transferred on a Hybond XL membrane (GE Healthcare, 2 mA/cm^2 of membrane) for 1 h. The membrane was air-dried for 20 min, blocked with 2 % skimmed milk in PBS over-night at 4 °C, and washed with BB:PBS (1:2) for 40 min. Detection was performed with 6338 (20 µg/mL in BB:PBS (1:2)) for 1 h at RT. The membrane was washed 3× for 10 min with 0.1 % of PBS-T, 1× with water, before secondary detection and visualization was performed using Strep-Tactin IR800 as described above. A size estimation of the stained heparosan was achieved using the Select-HA^{Tm} Lo-Ladder marker (tebu-bio GmbH, see 2.1).

The determination of an EC_{50} for the binding of 6338 to immobilized heparosan was performed using an ELISA-based assay adapted from Schwarzer et al. (2009). ELISA plates (96-well, MaxiSorp, ThermoScientific) were incubated with 50 ng of unfractionated heparosan dissolved in 50 µL of PBS over-night at 4 °C. Blocking solution (100 µL of 1 % BSA (Sigma Aldrich), 0.05 % PBS-T) was added to each well for 1 h at RT and subsequently removed by washing with 200 µL of PBS. Construct 6338 (19–25 µg/mL in 50 µL blocking solution) was added for 1 h at RT and subsequently unbound 6338 was removed by washing 3× with 200 µL of 0.1 % of PBS-T. Detection of the Strep-tag II in 6338 was achieved with StrepTactin® coupled to horseradish peroxidase (StrepTactin® conjugate, IBA, 1:4000 dilution in 50 µL of blocking solution, 1 h at RT). Unbound StrepTactin® conjugate was removed by washing with PBS-T and PBS (3× each, 200 µL) prior to development with ABTS (2,2-Azino-di[3-ethylbenzthiazolinsulfonat, Boehringer) according to the manufacturer's guidelines. Normalized absorption (405 nm) averaged from 3 to 9 experiments was plotted against iKflB concentration and hyperbolic fits to the data were used to calculate EC_{50} values (Origin 2020b software, OriginLab Corporation). The error bars report standard deviation.

2.11. Microscale thermophoresis

The interaction of unfractionated heparosan, fractionated heparosan (F31–35, see Supplementary Fig. S6), hyaluronan and heparan sulfate with iKflB was assessed by microscale thermophoresis (Wienken et al., 2010). The fluorescence signal of eGFP fused to iKflB was used to follow complex formation and movement of complexes in the applied temperature gradient. Microscale thermophoresis was performed in premium glass capillaries (NanoTemper Technologies, Monolith NT.115, #MO-K025), loaded with 20 nM of eGFP-iKflB and increasing concentrations of the aforementioned ligands in assay buffer (25 mM Tris pH 8.0, 50 mM NaCl) with 0.05 % Tween-20. Thermophoresis was induced with infrared-laser power set to 60 %. eGFP fluorescence was excited with the blue LED channel at 100 % power on a Monolith NT.115Nano device (NanoTemper Technologies). Normalized thermophoresis fluorescence averaged from 3 to 4 experiments was plotted against ligand concentration and hyperbolic fits to the data were used to calculate KD values (Origin 2020b software, OriginLab Corporation). The error bars

report standard deviation.

2.12. Staining of CHO cells

Chinese Hamster Ovary (CHO) cells and pgsA745 mutant cells (Δ*XylT2*) (Esko et al., 1985) were grown on coverslips for 2 days. After brief washing in PBS, the cells were fixed in 4 % paraformaldehyde in PBS for 30 min. Cells were blocked with 0.1 % BSA in PBS and stained using Strep-eGFP-iKflB (6338, 1 μg/mL) and mouse monoclonal antibody 10E4 (2 μg/mL, Amsbio), for which Alexa-Fluor-568 goat-anti-mouse IgM (2 μg/mL Invitrogen) was used as secondary antibody, in PBS with 0.1 % BSA. Cells were stained for 5 min in 1.25 μg/mL Hoechst 33258 in PBS and transferred to microscope slides with DAKO fluorescence mounting medium. Images were acquired using a Zeiss Axio Observer Z1 microscope using a 63× oil objective. Exposure times were equal for WT and mutant CHO cells, 0.2 s for the blue (Hoechst 33258), 4 s for the green (GFP) and 0.2 s for the red (Alexa 568) channel.

3. Results

3.1. Generation of a fluorescently labeled heparosan oligomer

Our first aim was to investigate if the K5 heparosan synthases, KfiA and KfiC, can generate fluorescently labeled heparosan of low dispersity and different sizes starting from a fluorescently labeled oligomeric acceptor. To produce such an acceptor, we exploited a previously described *E. coli* K-12 derivative, which produces short heparosan oligomers by expressing the K5 capsule biosynthesis genes together with the heparosan lyase *elmA* (Barreteau et al., 2012) (Supplementary Table S1). ElmA depolymerizes heparosan by catalyzing a β-elimination reaction at C-4 of GlcA, which cleaves the glycosidic bond and yields a Δ4,5-unsaturated GlcA moiety at the non-reducing end of the polysaccharide chain. The introduced double bond allows product detection at λ = 232–250 nm and enabled us to monitor the size fractionation of the oligosaccharides by SEC (Fig. 1A-C). Mass spectrometry (Supplementary Fig. S1) was used to determine the chain length of the obtained K5 oligosaccharides (Fig. 1C). The K5 Δ-decamer 1 (K5 oligosaccharide decamer carrying a Δ4,5-GlcA moiety) was the dominant species in the mixture (see Fig. 1C), was likely of sufficient size for enzymatic

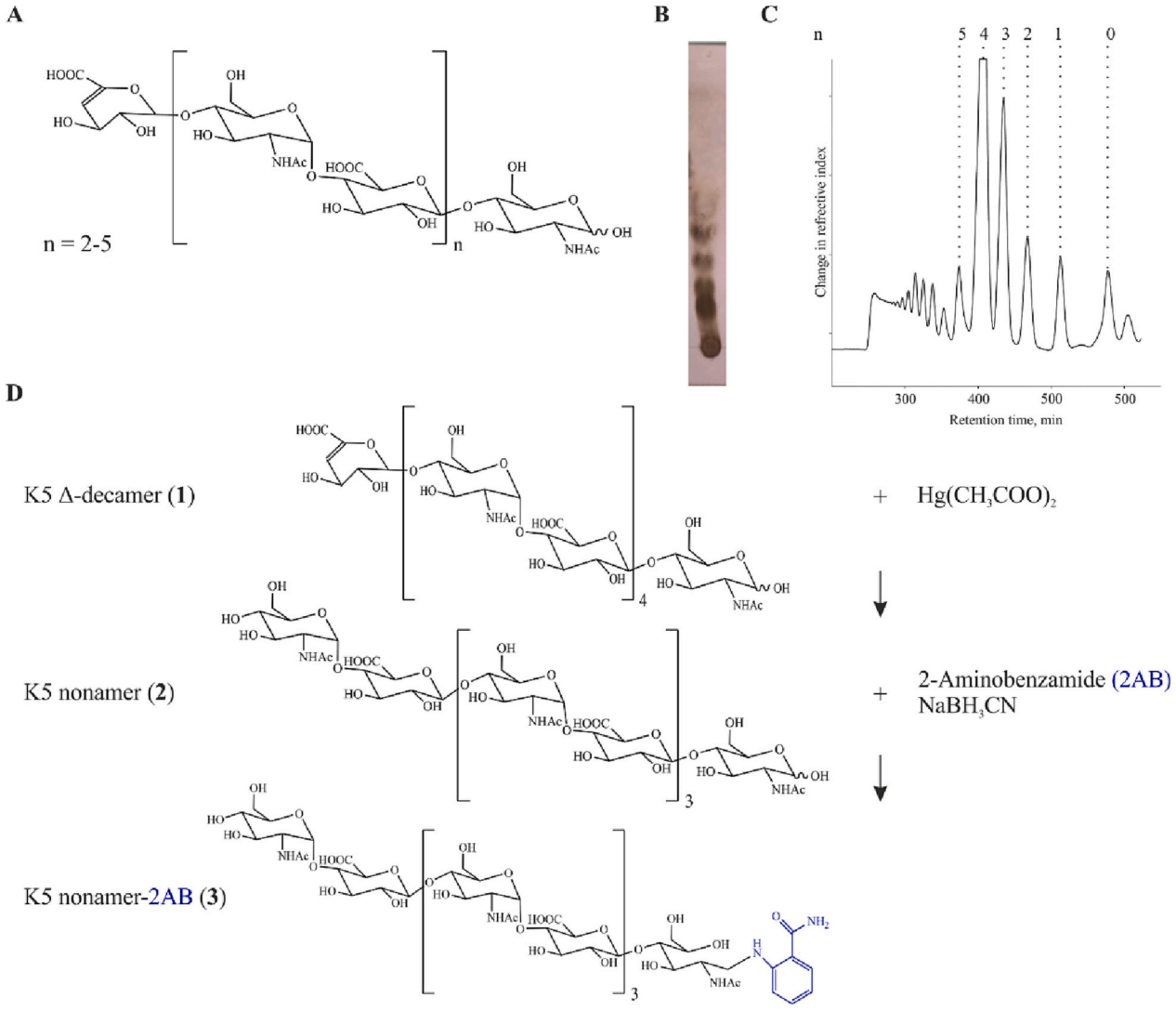

Fig. 1. Generation of a fluorescently labeled heparosan nonamer. (A) Structure of heparosan (K5) oligosaccharides harvested from bacterial cultures (Barreteau et al., 2012), n represents the number of internal GlcNAc-GlcA repeating units. Note the double bond introduced by ElmA (Barreteau et al., 2012). (B) Thin layer chromatogram of the harvested K5 oligosaccharides and (C) corresponding size exclusion chromatogram. (D) Schematic representation of the strategy utilized to produce the 2AB labeled K5 nonamer **3**.

elongation (Chen et al., 2006; Sugiura et al., 2010) and was thus chosen as a substrate for introducing a fluorescent label (Fig. 1D). To transform 1 into an oligosaccharide that is accessible for the enzymes, we selectively removed the Δ4,5-GlcA moiety in the presence of mercury (II) acetate (Ludwigs et al., 1987). This yielded the corresponding K5 nonamer 2, which carries a GlcNAc moiety at the non-reducing end. The reducing end of compound 2 was subsequently labeled with 2AB, resulting in the K5 nonamer 3. The identity of 3 was confirmed by mass spectrometry (Supplementary Fig. S1).

3.2. Investigation of the elongation mechanism of untagged KfiA and KfiC

To utilize KfiA and KfiC for biotechnological purposes, the enzymes should ideally elongate 3 in a distributive way. A hallmark of distributive elongation is a product population of low dispersity growing in size over time. In contrast, processive elongation yields long products at early time points of the reaction, and the dispersity is comparably high (Budde et al., 2020; Fiebig et al., 2018; Yakovlieva & Walvoort, 2020).

To characterize the elongation mechanism of KfiA and KfiC, we co-expressed both enzymes in *E. coli* using an arabinose-inducible system (pBAD, Supplementary Table S2 and S3). We used untagged proteins to exclude a possible interference of artificial peptide sequences with the elongation mode. The fluorescent tag on compound 3 enabled us to monitor KfiCA activity in the soluble fraction of bacterial lysates, making tag-based affinity purification dispensable. Using HPLC-based anion-exchange chromatography (AEC), we observed the elongation of 3 in the presence of UDP-GlcA and UDP-GlcNAc (Fig. 2A) in a time-dependent manner. Product sizes increased over time, yielding a Gaussian-shaped product population with low dispersity, indicating distributive elongation (Fig. 2B). This agrees with reports describing the elongation

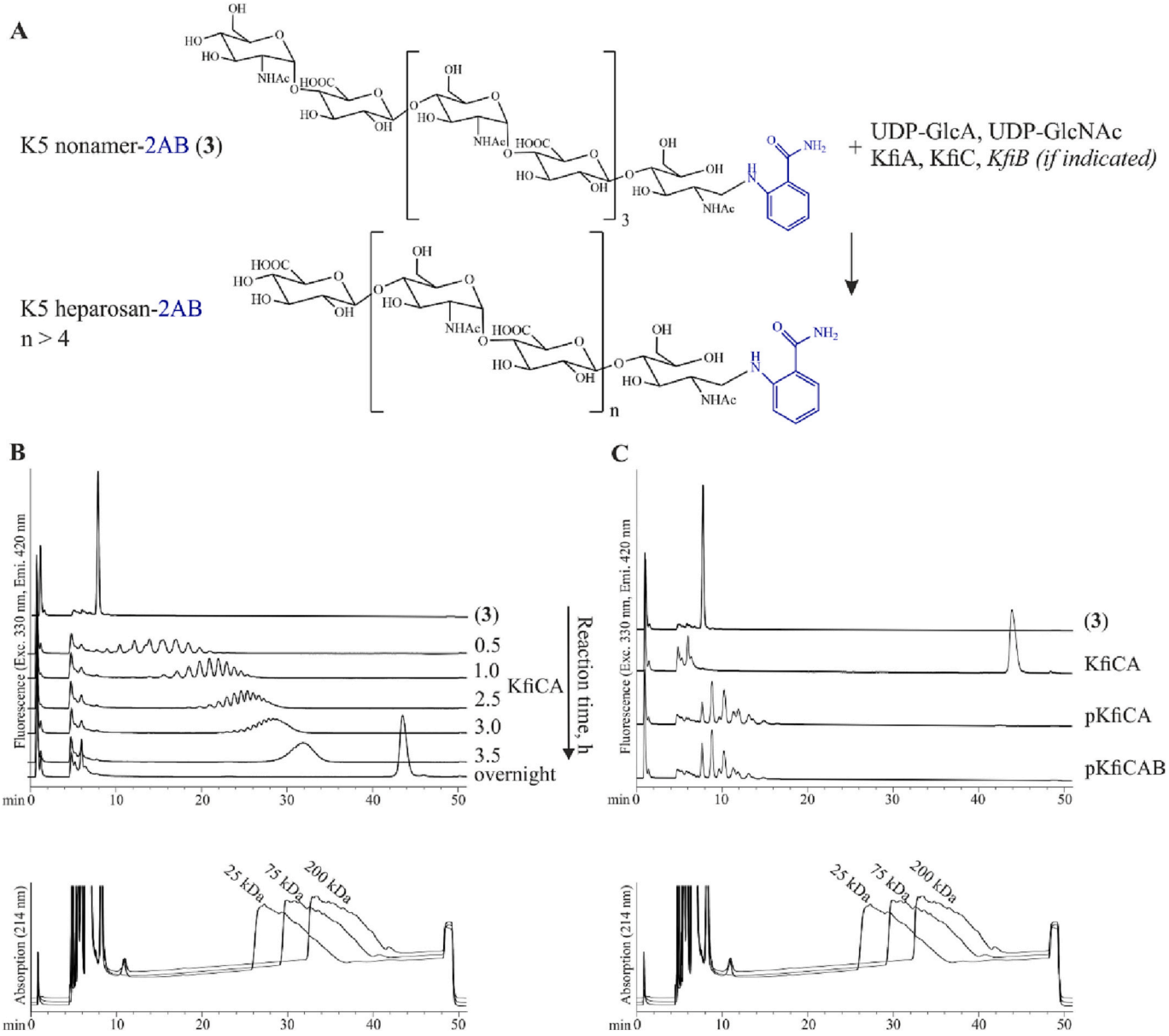

Fig. 2. Elongation of the 2AB labeled K5 nonamer and detection of products using HPLC-AEC (see 2.2 and 2.7). (A) Schematic representation of the reaction. (B, top chromatogram) Time-course of the elongation of K5 nonamer-2AB (**3**) by non-tagged KfiCA obtained from expression culture lysates. (C, top chromatogram) Elongation of the K5 nonamer-2AB (**3**) by tagged and purified pKfiCA, pKfiCAB, and non-tagged KfiCA (from panel B) after overnight incubation. (B, C, bottom chromatograms) Commercially available hyaluronan standards (Select-HA^{Tm} 25 k, Select-HA^{Tm} 75 k and Select-HA^{Tm} 200 k) ranging in size between 18 and 33 kDa, 68–83 kDa and 180–220 kDa, respectively, were used to calibrate the HPLC-AEC gradient. Heparosan polymers generated by KfiCA overnight elute later than hyaluronan polymers with a M_W of 220 kDa. The signal intensity of all three chromatograms was decreased for illustrative purposes.

mechanism of homologous GAG polymerases from *Pasteurella multocida* (Jing & DeAngelis, 2004; Sismey-Ragatz et al., 2007). After overnight incubation, heparosan polymers with an average molecular weight (avMw) > 220 kDa could be detected (Fig. 2B).

3.3. Evaluating tagged and purified KfiA and KfiC constructs for the synthesis of heparosan

Besides size control, one of the essential advantages of the enzyme-based in vitro production of heparosan is the purity of the catalysts and substrates, which reduces the effort for downstream processing of the polymer (DeAngelis et al., 2013). To enable enzyme purification, KfiA and KfiC were cloned as tagged fusion constructs with an N-terminal hexa-His-tag, and as a fusion protein with the chaperone trigger factor (TF), respectively, forming the previously described constructs (Sugiura et al., 2010) His_6-KfiA and His_6-TF-KfiC (hereafter referred to as pKfiA (5644) and pKfiC (5822), see Supplementary Table S2 and Supplementary Fig. S2). pKfiA and pKfiC could be enriched from expression culture lysates with a yield (1.2 mg/L culture and 12.8 mg/L culture, respectively) and purity sufficient for subsequent experiments (Supplementary Fig. S3A, Supplementary Table S4). The acceptor 3, ending with GlcNAc, allowed us to confirm that pKfiC was only active in the presence of pKfiA (Sugiura et al., 2010) (Supplementary Fig. S3B) and that both purified enzymes act in concert as polymerases. However, a direct comparison between the chain length achieved with pKfiCA, and the products synthesized by non-tagged constructs from culture lysates, demonstrated that the latter produced considerably larger chain lengths (Fig. 2C).

Since KfiB has previously been reported as a scaffolding factor (Cress et al., 2014; Hodson et al., 2000; Zhang et al., 2012), we hypothesized that it might stabilize KfiA and/or KfiC, promoting the production of longer heparosan chains. Therefore, we cloned and purified (5.2 mg/L) MBP-KfiB-His_6, in which KfiB was fused to maltose binding protein (Supplementary Fig. S3A). However, we could not observe the production of longer chains in the presence of pKfiB (Fig. 2C).

The reason for the impaired ability of pKfiCA to produce long chains is currently unclear. In case of the capsule polymerase of *Neisseria meningitidis* serogroup B, stability and activity issues of the recombinant epitope-tagged enzyme have been successfully addressed by directed evolution (Keys et al., 2012; Keys et al., 2014). This involved the expression of large enzyme libraries and the application of a polysaccharide-specific antibody for product detection. So far, however, the low immunogenicity of heparosan impeded the generation of selective, high-affinity antibodies (DeAngelis, 2015; Kizer et al., 2018), and anti-K5 antibodies that were available to us cross-react with ubiquitous surface molecules (Peters et al., 1985). To fill the current gap in heparosan-specific detection tools, we characterized a phage-borne heparosan-degrading enzyme, eliminated its catalytic properties and transformed it into a heparosan-binding protein.

3.4. Expression and purification of the ΦK5B tailspike protein KflB

Partial sequencing of the genome of ΦK5B, a so far uncharacterized *E. coli* K5-specific bacteriophage, revealed an open reading frame (ORF, Supplementary Fig. S4) that shows sequence similarity to known heparosan lyases. The respective gene product, which we termed KflB, shares 97.9 % sequence identity with the K5-lyase from ΦK1–5 (GenBank AAG59821.1 (Scholl et al., 2001)), 98.3 % sequence identity with the revised sequence of the K5-lyase KflA from ΦK5A (CAA71133.2, (O'Leary et al., 2013)), and 56.6 % sequence identity to ElmA from *E. coli* K5 (CAA65353 (Legoux et al., 1996)). Like these previously described K5-lyases, KflB encompasses a C-terminal sequence stretch with sequence similarity to the C-terminal, intramolecular chaperone domain (CTD) found in endosialidases (endoN) and several other bacteriophage tailspike, tail fibre and neck appendage proteins (Schulz et al., 2010; Schwarzer et al., 2007). To investigate if KflB can be expressed as a recombinant protein in *E. coli*, the ORF was amplified and cloned with N-terminal Strep II and C-terminal His_6-tag (Fig. 3A). In parallel, we designed a construct (KflB-S505A) to target the catalytic serine (S505) most likely involved in the autocatalytic cleavage of the CTD of KflB (Fig. 3B). KflB wt and KflB-S505A were expressed in *E. coli* BL21(DE3), purified via affinity chromatography, and analyzed using SDS-PAGE and Western blotting (Fig. 3C, D). Since TSPs can be SDS-resistant (Mühlenhoff et al., 2003), samples were analyzed with (+) and without (−) denaturation (95 °C for 5 min) prior to SDS-PAGE. Denatured KflB wt migrated with the expected molecular weight of a mature monomer (54 kDa), while the shift of KflB-S505A was consistent with a retained CTD (16 kDa). The His_6-tag (Fig. 3D, red channel) located at the C-terminus of the CTD was only detectable by Western Blot in KflB-S505A, corroborating that S505 is required for the autocatalytic loss of the CTD. When the denaturation step was omitted, species of higher molecular weight (~150 kDa and ~130 kDa for KflB wt and KflB-S505A, respectively) were detectable by Coomassie-staining but not visible in the corresponding Western blot directed against the N-terminal Strep-tag II (compare Fig. 3C, yellow box, with Fig. 3D, green channel, 150 kDa), suggesting that the N-terminal tag might be buried inside an enzyme complex. The increased apparent molecular weight is consistent with KflB wt forming a homotrimer and agrees with the observation of a trimer in the crystal structure of KflA (Thompson et al., 2010). As observed for the S991A mutant of endoNF (Schwarzer et al., 2007), the retained CTD impacts trimer formation and thus migration of KflB-S505A during PAGE.

3.5. KflB is a heparosan lyase

We investigated if KflB exhibits heparosan lyase activity. Heparosan from metabolically engineered *E. coli* BJ (Barreteau et al., 2012; Leroux & Priem, 2016) was purified, fractionated, characterized (Supplementary Fig. S6), incubated with KflB, and samples were taken at different time points. To elucidate if the presence of the CTD impacts enzyme activity, we included KflB-S505A in the experiment. Products were separated and visualized on a PA (polyacrylamide) gel stained with Alcian blue/silver (Fig. 4A, C) and using an HPLC-based anion-exchange chromatography (AEC) assay with UV detection (Fig. 4B, D). Both assays demonstrated that the constructs were active, which agrees with earlier studies showing that the loss of the CTD of TSPs is not required for maturation into an active enzyme (Mühlenhoff et al., 2003; Schwarzer et al., 2007).

Interestingly, KflB leaves a mixture of four short oligosaccharide products as detected by HPLC-AEC (Fig. 4B, D). Thus, we investigated the minimal substrate size of KflB using the oligosaccharides shown in Fig. 1C. The K5-derived tetramer ($n = 1$, see Fig. 1A), hexamer ($n = 2$), octamer ($n = 3$) and decamer ($n = 4$) were incubated in the presence of KflB wt. HPLC-AEC (Fig. 5) demonstrated degradation of the deca-, octa-, and hexamer into mixtures of shorter oligomers, while the tetramer remained unchanged. Therefore, we concluded that the minimal length of the substrate for KflB would be a hexamer (n = 2, see Fig. 1A). These results are in agreement with published literature that reported hexaoctamers of heparosan as a minimal substrate for KflA (Murphy et al., 2004; O'Leary et al., 2013).

3.6. Analyzing the degradation mode of KflB using 2AB-K5 heparosan as substrate

It is still a matter of debate if heparosan lyases utilize an exolytic (exo) or an endolytic (endo) mode of degradation (Hänfling et al., 1996; Murphy et al., 2004; O'Leary et al., 2013; Thompson et al., 2010). The 2AB-labeled heparosan generated by KfiCA (see Fig. 2B) was of high molecular weight and low dispersity, enabling us to investigate the mode of action of KflB. An ideal exo lyase would cleave off small unlabeled fragments of the non-reducing end (which faces away from the bacterial membrane in the in vivo situation (Sande & Whitfield, 2021;

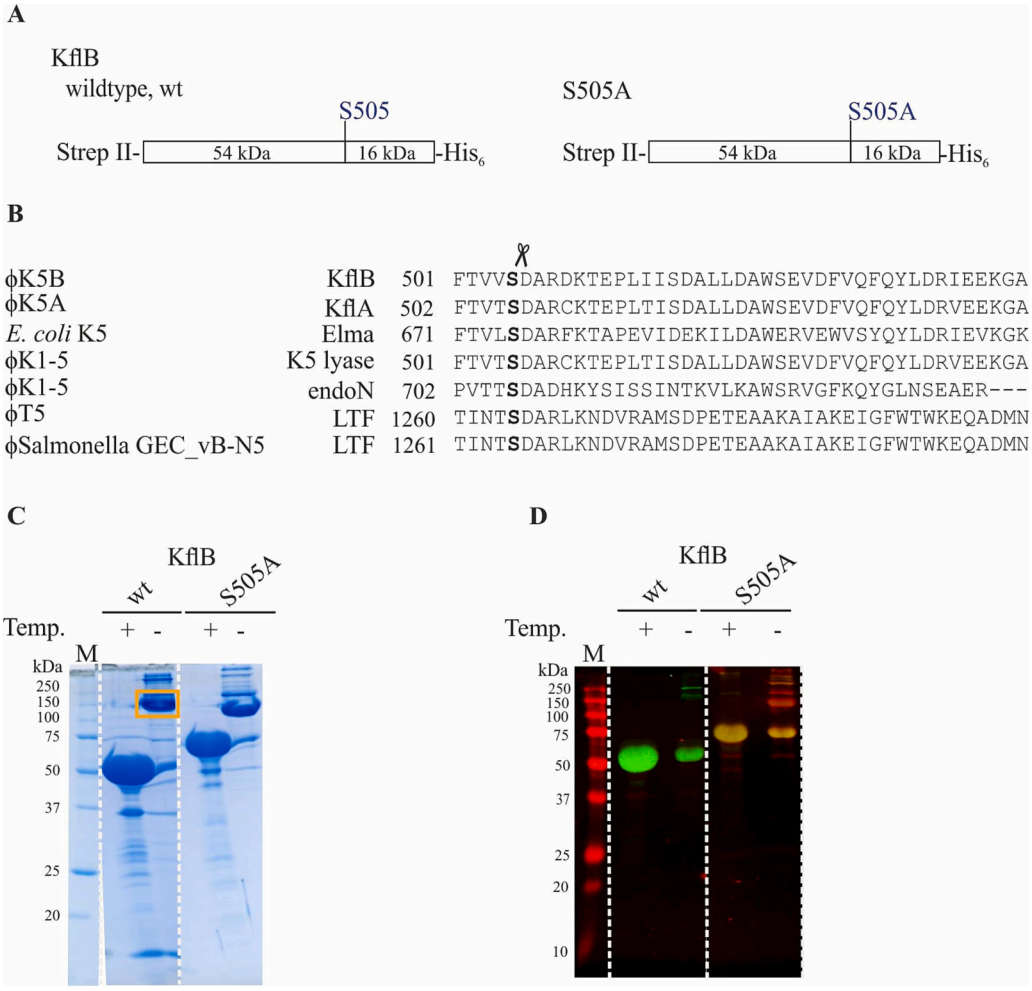

Fig. 3. Recombinant expression of KflB. (A) Schematic representation of KflB wild-type and KflB-S505A. (B) Partial multiple sequence alignment of tailspike proteins harboring a C-terminal chaperone domain (CTD). From the left: the origin of the protein, name of the protein, number of the first residue included in the alignment, and amino acid sequence. The conserved serine residue is marked in bold. The scissors (SerAsp) indicate the proteolytic cleavage site. The multiple sequence alignment was generated by Clustal 2.1 using proteins of the following accession numbers (European Nucleotide Archive database): CAA71133 (KflA), CAA65353 (Elma), AAG59821 (K5 lyase), AAG59822 (endoN), CAJ29339 (L-shaped tail fibre protein LTF of coliphage T5), QPI15176.1 (Long tail fibre LTF of the salmonella phage GEC_vB_N5). (C) Gel from SDS-PAGE stained with Coomassie Brilliant Blue G-250 (Roth) showing purified Strep II-KflB wt and Strep II-KflB-S505A. The whole gel is shown in Supplementary Fig. S5. The SDS-resistant complex of Strep II-KflB wt is marked by an orange box. (D) Corresponding Western Blot analysis. Strep II-tag (green channel), His_6-tag (red channel). M – marker, T - temperature, "+" – denatured samples. (For interpretation of the references to colour in this figure legend, the reader is referred to the web version of this article.)

Willis et al., 2013; Yan et al., 2020)) of 2AB-K5 heparosan, resulting in a population of polymers that slowly decreases in size over time. In contrast, an ideal endo lyase would cut the polymer at random locations without bias, leading to a broad product spectrum of labeled and unlabeled products with short oligomers present from the start and accumulating at later time-points of the reaction. The KflB-catalyzed degradation of 2AB-K5 heparosan was monitored using HPLC-AEC with fluorescence detection (Fig. 6), demonstrating that the starting material disappeared rapidly, leaving products of high dispersity, which were further degraded over time. These observations are in very good agreement with an endolytic mode of action.

3.7. Characterization of KflB substrate specificity

The development of molecular tools for engineering GAGs is of great interest (DeAngelis et al., 2013; Miller et al., 2014). GAGs are very stable and require harsh conditions to undergo chemical degradation, whereas enzymatic degradation is performed under mild conditions, representing an appealing alternative (Bohlmann et al., 2015; Miller et al., 2014; Murphy et al., 2004). Consequently, we investigated if KflB was capable of degrading other GAGs. KflB wt was incubated with heparosan (unfractionated, Supplementary Fig. S6), and commercially available hyaluronan, heparan sulfate, chondroitin sulfate, and dermatan sulfate (see 2.1 for details). Products were analyzed using PAGE combined with Alcian blue/silver staining (Fig. 7). As expected, heparosan was completely degraded already after 0.5 h. Hyaluronan, chondroitin sulfate, and dermatan sulfate, which are structurally different from heparosan (DeAngelis et al., 2013), were resistant to KflB digestion. Heparan sulfate was slightly degraded within half an hour of incubation, but longer incubation times did not change the product profile. It is tempting to speculate that heparan sulfate is a substrate for KflB due to its structural similarity to heparosan (see Discussion) (Chen, Li, et al., 2013; DeAngelis et al., 2013).

3.8. Identification of KflB's active center

Stummeyer et al. demonstrated the possibility of transforming the TSP endoNF into a polysialic acid detection agent (Stummeyer et al., 2005). Active site mutations led to the loss of endosialidase activity, while the resulting constructs retained their affinity towards polysialic acid, most likely via a separate binding site present in the stalk domain of this enzyme (Schwarzer et al., 2009; Stummeyer et al., 2005). Therefore, we investigated if KflB can be transformed into a heparosan detection agent. Thompson et al. determined catalytically essential residues in KflA based on its apo structure (Thompson et al., 2010). A multiple sequences alignment identified F202, E206, K208, and Y229 as corresponding residues in KflB (Fig. 8A). Using site-directed mutagenesis, we introduced single or double amino acid exchanges to alanine in KflB, purified the resulting constructs (Supplementary Fig. S5) and analyzed their activity towards heparosan in an overnight reaction. Heparosan was included as a control in the absence of the enzyme. The reactions were analyzed by Alcian blue/silver stained PAGE (Fig. 8B). As expected, incubation with KflB wt led to the complete degradation of heparosan. Surprisingly, all single amino acid exchange mutants showed residual activity (Fig. 8B, compare product profile to heparosan control). Activity of double amino acid mutants was drastically reduced (Fig. 8B).

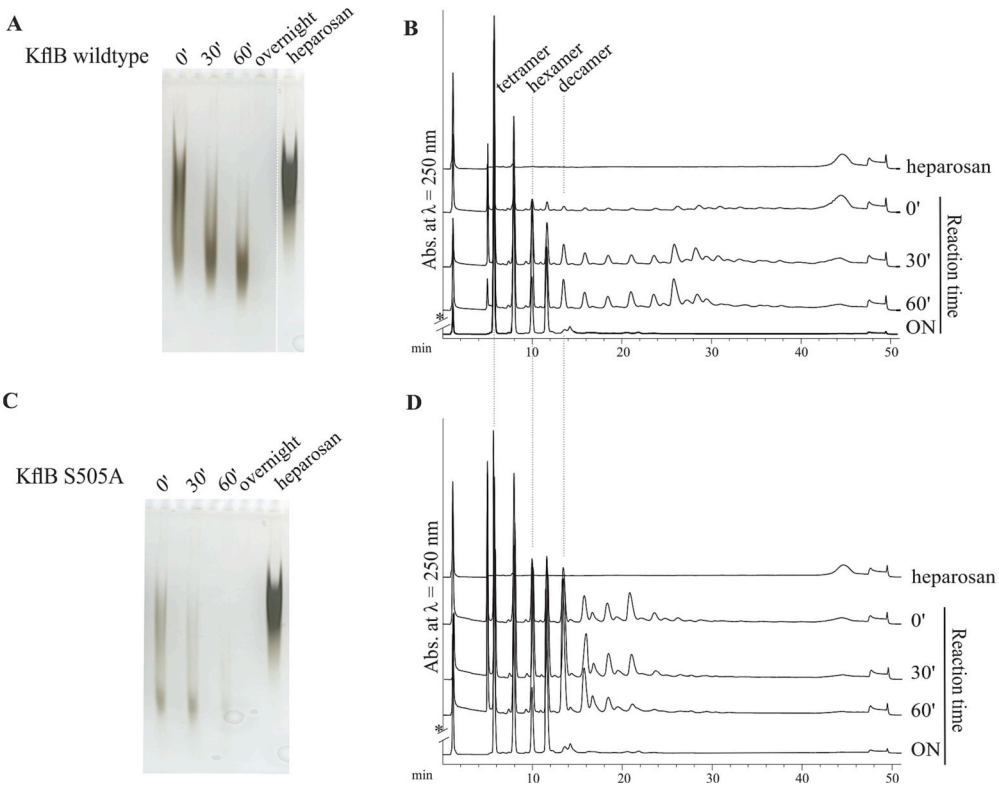

Fig. 4. Enzymatic activity of KflB. Heparosan (F27–30, see Supplementary Fig. S6) degradation catalyzed by KflB wt (A, B) and KflB S505A (C, D). Products were visualized after (A, C) PAGE by Alcian blue/silver staining or (B, D) by UV detection after separation by HPLC-AEC (see 2.8.1). The HPLC-AEC gradient used in (B, D) was calibrated with the heparosan oligomers shown in Fig. 1C, which allowed assigning the degree of polymerization to the product peaks. *The signal intensity of the overnight (ON) sample was decreased for illustrative purposes. (For interpretation of the references to colour in this figure legend, the reader is referred to the web version of this article.)

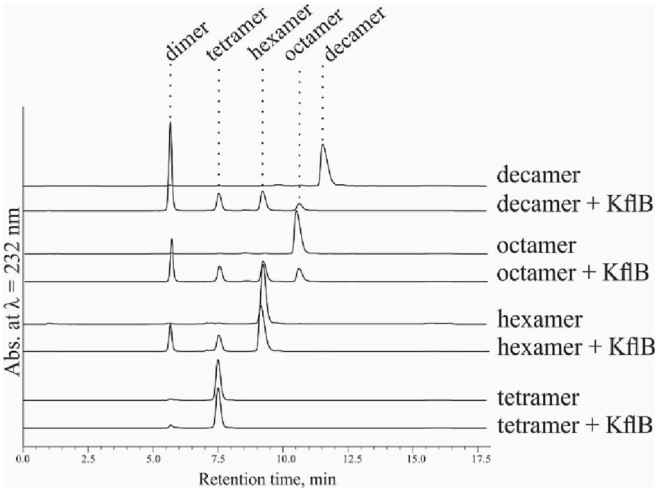

Fig. 5. The minimal substrate for KflB. Heparosan oligomers in the presence and absence of KflB after overnight incubation. Products were analyzed via HPLC-AEC coupled to UV detection (see 2.8.2). The identity of the starting material was confirmed by MS analysis (Supplementary Fig. S1).

To better evaluate the extent of remaining activity in constructs with one and two amino acid exchanges, KflB wt, KflB-E206A and KflB-E206A, K208A were incubated with unfractionated heparosan and lyase activity was monitored over-time by following the degradation of heparosan using PAGE followed by Alcian blue/silver staining (Fig. 8C-E). During the first 3 h of the reaction, heparosan was slightly reduced in size by KflB-E206A (Fig. 8D). In contrast, the size of heparosan was not affected by the presence of KflB-E206A, K208A during that timespan (Fig. 8E), emphasizing that the lyase activity of the construct is sufficiently reduced for its use in e.g. blots or ELISA assays, for which incubation times are usually shorter than 3 h (see methods).

3.9. Development of a heparosan detection agent

All double amino acid exchange mutants were unsuccessfully screened for their suitability as detection agents on *E. coli* K5 cells, most likely due to the poor accessibility of the Strep-tag II (see also Fig. 1D). As a minor degree of heparosan detection was possible using inactive KflB-E206A, K208A (hereafter referred to as iKflB), we decided to optimize the N-terminus of this construct for detection by introducing various linkers and/or fusion tags. To improve the readability, we refer to the constructs using their identifiers, as shown in Fig. 9 and Supplementary Table S2. Constructs were generated according to the following rationale: (I, 6223) an ALFA-tag (Götzke et al., 2019) was introduced between Strep-tag II and KflB's N-terminus to expose the Strep-tag II and to allow an additional possibility of detection via the anti-ALFA antibody; (II, 6224) an ALFA-tag was introduced near the S505 cleavage site to have a C-terminal tag after the loss of the CTD; (III, 6336) a flexible GS24 linker (Chen, Zaro, & Shen, 2013) was introduced in 6223 between the ALFA-tag and the enzyme's N-terminus to further expose the tags; (IV, 6338) KflB was N-terminally fused to Strep II-eGFP-GS24 (enhanced green fluorescent protein) for better exposure of the Strep-tag II and to enable detection via green fluorescent protein if required; (V) iKflB (construct 6168) was directly labeled with a fluorescent dye yielding iKflB-IR800. All constructs except for 6224 could be purified (Supplementary Table S4). Interestingly, the ALFA-tags could not be detected in a Western Blot in any of the constructs (not shown). Only the Strep-tag II of the eGFP fusion protein 6338 (hereafter referred to as Strep-eGFP-iKflB) could be visualized without prior denaturation, indicating that it is not buried inside the enzyme and thus might be accessible (Fig. 9B).

3.10. Characterization of iKflB

We performed dot blots with strains obtained from liquid bacterial cultures to determine the applicability of Strep-eGPF-iKflB (6338) and iKflB IR800 for detecting heparosan on bacterial surfaces. More

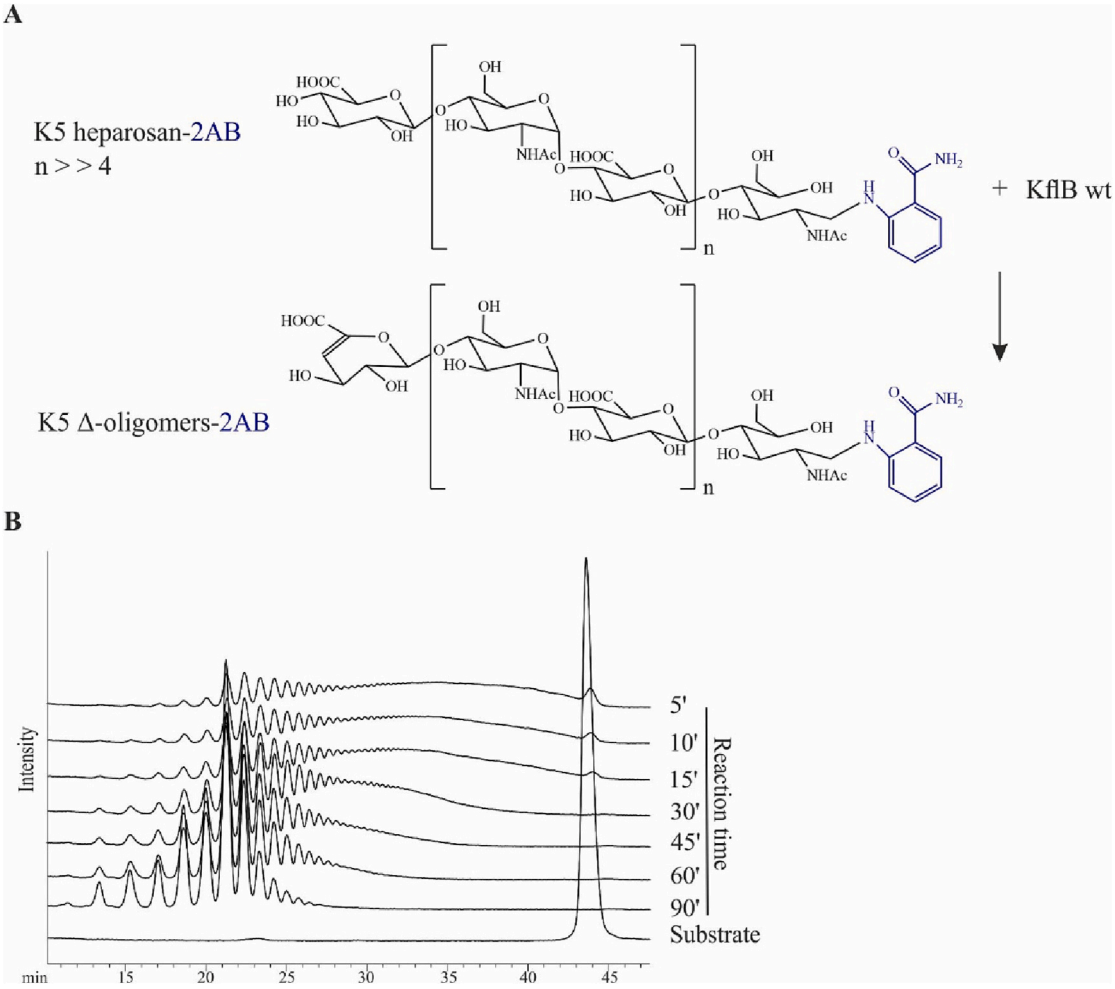

Fig. 6. Depolymerization of fluorescently labeled heparosan by KflB. (A) Schematic representation of the reaction. (B) Time-course of the reaction with separation and detection of 2AB labeled substrates and products by HPLC-AEC (see 2.8.1).

specifically, we included *E. coli* K5 as a natural heparosan-producing strain and an engineered *E. coli* BJ derivative (Leroux & Priem, 2016) carrying pBAD33-kfiCAB (5744, see Supplementary Table S2) and pBBR3-kfiD (5691) to simulate a directed evolution experiment (Keys et al., 2012). *E. coli* BJ was included as a control, and *E. coli* K1, a polysialic acid-producing strain, was used to exclude the possibility of unspecific binding to a negatively charged capsule polymer. Both constructs, Strep-eGPF-iKflB (6338) and iKflB IR800, could be exploited to detect heparosan on *E. coli* harvested from bacterial cultures (Fig. 10A, B), while both controls clearly remained negative, suggesting that iKflB might be a valuable tool for serotyping or for the directed evolution of heparosan polymerases.

Schwarzer et al. developed an ELISA-based assay to characterize the binding of various inactive endoNF mutants to polysialic acid and determined EC_{50} values (protein concentration of half-maximal binding) for each construct (Schwarzer et al., 2009). We adapted this assay and found that half-maximal binding of Strep-eGPF-iKflB (6338) to the wells coated with unfractionated heparosan was obtained at a concentration of 50 nM or 4.15 µg/mL (Fig. 11A). The titration shown in Fig. 11A was used as guidance for choosing a working concentration (3-5× EC_{50}) for iKflB in the following assays.

To determine the detection limit for heparosan on a nitrocellulose membrane, a serial dilution of unfractionated heparosan (avMW = 100 kDa, characterized in Supplementary Fig. S6) ranging from 15.4 µg – 0.48 µg was spotted and detection was achieved either directly using fluorescently labeled iKflB-IR800 or indirectly using Strep-eGFP-iKflB (6338) followed by fluorescently labeled Strep-Tactin IR 800 (Fig. 10C). Fig. 10C shows that 0.48 µg and 0.96 µg of polymer were still detectable using iKflB-IR800 and Strep-eGFP-iKflB (6338), respectively. A similar sensitivity was observed for the hyaluronan binding protein aggrecan and the detection of Select HA^{Tm} (avMW = 70 kDa) using vacuum slot blotting (Yuan et al., 2013).

The dot blot was also utilized to investigate if commercially available GAGs would be recognized by iKflB, but only heparosan could be detected (Fig. 10D).

To obtain additional information about cross-reactivity with other GAGs, but also about the size of heparosan being detectable on a membrane using iKflB, the polymers were separated via PAGE (Litschko et al., 2021) and then transferred onto a positively charged nylon membrane using electro-transfer blotting. Detection was achieved using Strep-eGPF-iKflB (6338) followed by Strep-Tactin IR800. Again, only heparosan was detectable (Fig. 10E). To corroborate that all GAGs were transferred, the nylon membrane shown in Fig. 10E was additionally stained with Alician blue (Fig. 10F). Interestingly, the unfractionated heparosan was not detectable, presumably, because the detection limited for staining unsulfated GAGs with Alcian blue on a membrane is up to five times higher than for sulfated GAGs (Volpi & Maccari, 2015). In addition to the gel used for blotting (Fig. 10E, F), a second gel was run in parallel (using the same electrophoresis chamber) and was subsequently stained with Alcian blue/silver (Fig. 10G). Besides the GAGs, this gel contained Select-HA^{Tm} Lo-Ladder to evaluate the size of the polymers. A comparison between blot and gel reveals that only

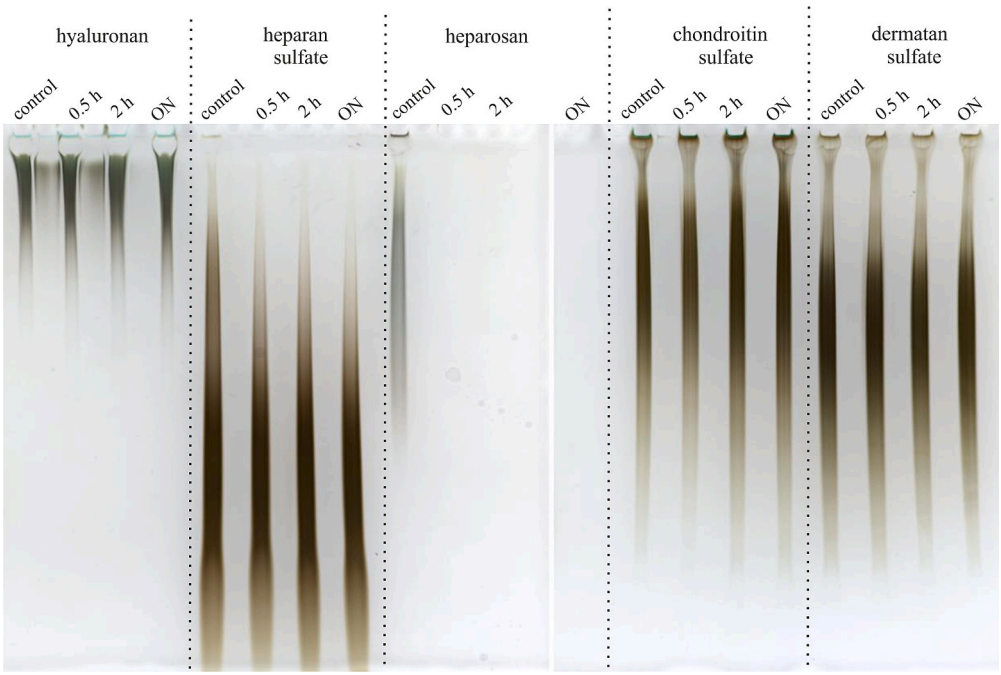

Fig. 7. KflB substrate specificity. Different glycosaminoglycans were incubated with KflB and analyzed after the indicated time points using PAGE, followed by Alcian blue/silver staining. A control reaction in the absence of KflB was incubated overnight to document the stability of the respective polymer in the reaction buffer. (For interpretation of the references to colour in this figure legend, the reader is referred to the web version of this article.)

heparosan with a Mw > 20–30 kDa is detectable using iKflB. It is important in this context that Yuan et al., 2013 observed the same Mw-dependence for the detection of hyaluronan after electro-transfer blotting, using either aggrecan or Alcian blue, and demonstrating that the effect is not an inherent feature of the detection agent (Yuan et al., 2013). It is of note that heparosan and hyaluronan are not modified and structurally very similar. Thus, a size comparison based on electrophoretic mobility should be reasonably accurate. In contrast, all other GAGs are sulfated and should thus have increased electrophoretic mobility, making a comparison to the hyaluronan standard inaccurate.

In all of the above described assays, iKflB was used to detect immobilized heparosan. We employed microscale thermophoresis to assess the interaction between Strep-eGFP-iKflB (6338) and unfractionated heparosan, fractionated heparosan (F31–35, see Supplementary Fig. S6), hyaluronan and heparan sulfate in solution. The iKflB concentration was held constant and the fluorescence signal of eGFP was used to follow complex formation. Taking into account that the smallest substrate for KflB consists of six monosaccharides (Fig. 5), we considered 10 monosaccharides (5 repeating units) as a realistic binding site for iKflB. Or in other words, we assume that e.g. a heparosan polymer with a chain length of 80 monosaccharides (16 kDa) would contain eight binding sites and could thus accommodate eight iKflB molecules. Consequently, the concentration of decameric binding sites is shown as ligand concentration in Fig. 11B, C and 0.52 ± 0.06 mM and 3.15 ± 0,75 mM were determined as K_D values for unfractionated heparosan and F31–35, respectively. As expected from the blot analyses above, no binding could be observed for hyaluronan and heparan sulfate, which were used as negative controls.

The purified heparan sulfate originating from porcine mucosa that we used in the blot assays (Fig. 10) was not detected by iKflB. This is not surprising, as mammalian heparan sulfate is highly sulfated (Merry et al., 2022) (80 %, as provided by the manufacturer). Interestingly, we observed that Strep-eGPF-iKflB recognizes an epitope on the cell surface of CHO cells (Fig. 12A). No such staining was detected on a xylosyltransferase 2-defficient CHO cell line (psgA-745, Δ*XylT2*) lacking proteoglycans and thus heparan sulfate (Cuellar et al., 2007; Esko et al., 1985) (Fig. 12D). Clear and identical staining was observed with Strep-eGPF-iKflB both alone (not shown) and in combination with the antibody 10E4 (Fig. 12C). The latter is a monoclonal that recognizes *N*-sulfated heparan sulfate (David et al., 1992). Antibody 10E4 does not stain mutant CHO cells either (Fig. 12E) and shows a heterogenous staining pattern on the whole cell surface (Fig. 12B). Binding of iKflB, on the other hand, is only observed in small segments of the cell surface that seem to be mainly in regions of cell-cell contact: This often, but not exclusively, corresponds to regions where 10E4 also shows strong staining (Fig. 12C). We hypothesize that patches of heparan sulfate seem to be present on the cell surface of CHO cells that have enough non-modified repeating units to be recognized by iKflB.

4. Discussion and conclusion

This study was based on the hypothesis that *E. coli* K5-based polymerases and lyases can broaden the toolbox for heparosan synthesis, depolymerization, and detection.

We could demonstrate that KfiA and KfiC can be used to synthesize heparosan of different sizes in vitro. They utilize a distributive elongation mechanism, which is ideal for biotechnological applications, as it offers control over the product size by adjusting the ratio between nucleotide sugar donor and acceptor (Yakovlieva & Walvoort, 2020). This agrees with studies demonstrating that homologous GAG capsule polymerases are distributive (Gottschalk et al., 2022; Jing & DeAngelis, 2004; Sismey-Ragatz et al., 2007). Processive group 2 polymerases usually harbor extended polymer binding sites sometimes located in separate domains (Budde et al., 2020; Cifuente et al., 2023; Fiebig et al., 2018; Keys et al., 2014). In agreement with our observations, no indication of such binding sites or domains has been found in bacterial GAG polymerases so far (Osawa et al., 2009), even though extended binding sites exist in viral enzymes with homologous function (Maloney et al., 2022).

Heparosan synthesis was successful in bacterial lysates using untagged KfiCA, whereas both the purity and the activity of the purified enzymes remained an issue. Thus, the *E. coli* K5 machinery is without

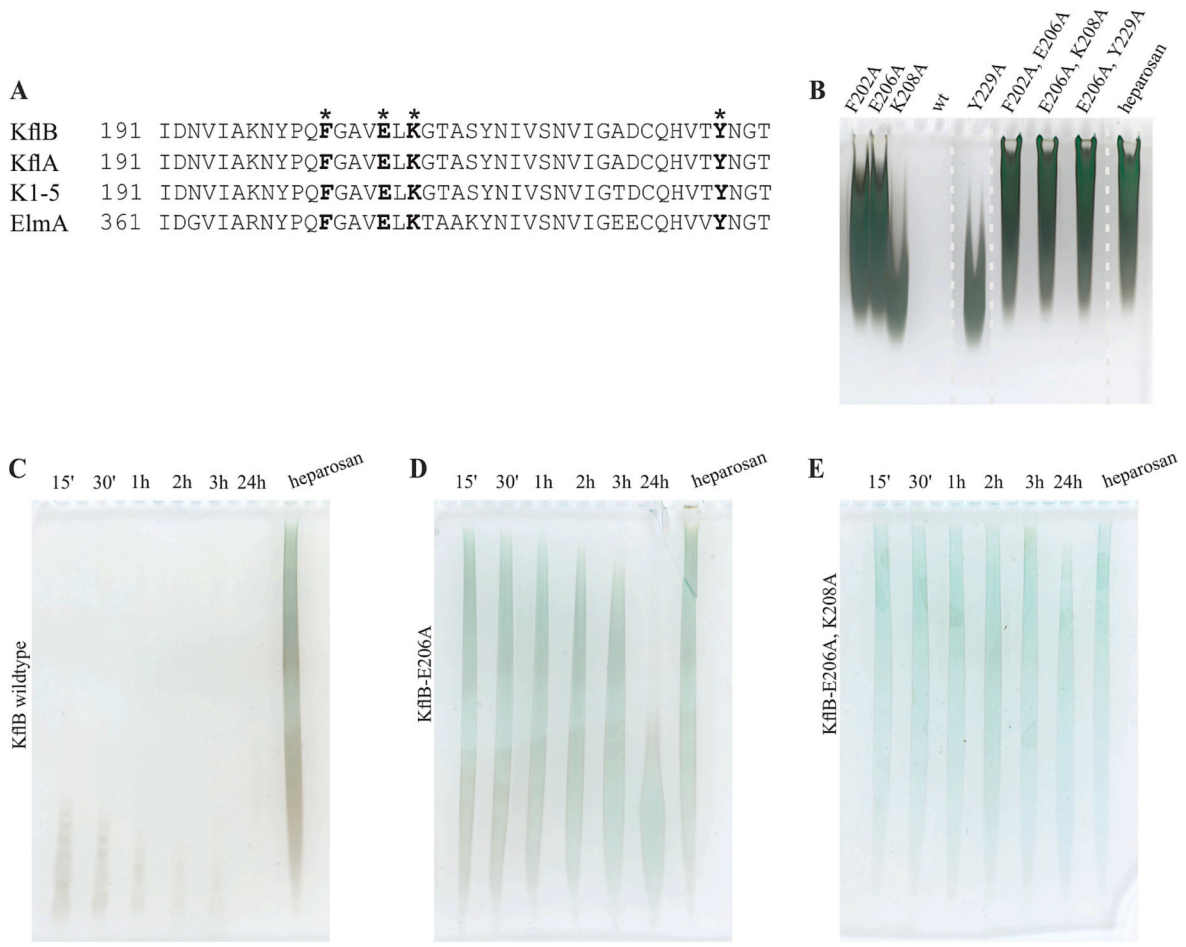

Fig. 8. Identification of active site residues in KflB. (A) Section of a multiple sequence alignment of heparosan lyases using the sequences as indicated in Fig. 3. From left to right: name of the protein, number of the first residue included in the alignment, amino acid sequence. Residues crucial for the activity of KflA (Thompson et al., 2010) are marked in bold. Residues marked with an asterisk were replaced by alanine resulting in the mutants shown in (B) Effect of recombinant KflB and its mutants on heparosan in overnight reactions. Products were visualized with Alcian blue/silver staining after PAGE. Heparosan incubated in the absence of the enzyme was used as a control. Recombinant KflB constructs and their identifiers: F202A (6112); E206A (6113); K208A (6114); wt (6118); Y229A (6119); F206A, E206A (6167); E206A, K208A (6168); E206A, Y229A (6169) (see Supplementary Table S2). (C-E) The ability to depolymerize heparosan was monitored over time for constructs KflB wt, KflB-E206A and KflB-E206A, K208A. Products were separated by PAGE and stained with Alcian blue/silver. Heparosan incubated in the absence of the enzyme was used as control. (For interpretation of the references to colour in this figure legend, the reader is referred to the web version of this article.)

further optimization inferior for in vitro synthesis to homologous enzymes, e.g. the heparosan synthases PmHS1 and PmHS2 from *Pasteurella multocida* (Chavaroche et al., 2012; DeAngelis & White, 2002, 2004; He et al., 2022; Otto et al., 2012). Interestingly, purified KfiA (in combination with KfiC homologs from *Pm*) has been successfully used for biotechnological purposes in vitro (Xu et al., 2011), whereas the expression of tagged KfiC was found insufficient for biotechnological applications (X. Zhang et al., 2019), even though considerable efforts for the optimization of reaction conditions and rational construct design (e.g., truncation studies) have been undertaken (Sugiura et al., 2010). The development of a detection agent for heparosan opens up the possibility of improving KfiA and KfiC activity and solubility by directed evolution (Keys et al., 2012, 2014), a method that has so far been inapplicable due to the lack of high-affinity antibodies suitable to screen large enzyme libraries without cross-reacting with common *E. coli* surface antigens (Peters et al., 1985).

The herein-developed detection agent is based on the newly identified TSP KflB. TSPs form oligomers and are attractive molecular tools because of their specificity for the target polymer and their high stability (Mühlenhoff et al., 2003), likely mediated by extensive contacts between the protomers (Thompson et al., 2010). Some TSPs, like the polysialic acid-degrading endoNF of ΦK1F, have distinct polymer binding sites located at a distance from the catalytic center (Stummeyer et al., 2005). This architecture might allow the phage to tightly bind to the host capsule while simultaneously degrading the polymer, ultimately reaching the bacterial membrane where infection occurs (Leiman et al., 2007). It further allowed developing inactive endoNF into a detection agent for polysialic acid (Kiermaier et al., 2016; Stummeyer et al., 2005). It is tempting to speculate that KflB or bacterial heparosan lyases in general exploit a similar binding site arrangement for binding to heparosan.

To characterize the binding between iKflB and heparosan, we performed microscale thermophoresis and an ELISA-based assay. The latter demonstrated half-maximal binding to immobilized heparosan at a concentration (EC_{50}) of 50 nM of iKflB. This is in good agreement to EC_{50} values obtained for various inactive endoNF constructs (Schwarzer et al., 2009), which have been used for the detection and immunoprecipitation of polysialylated proteins in later studies (Kiermaier et al., 2016). In contrast, the K_D determined by microscale thermophoresis for the interaction between iKflB and heparosan in solution is in the μM-mM range and thus higher than e.g. the K_D values reported for heparin-protein interactions (nM-μM) (Peysselon & Ricard-Blum, 2014).

A

Protein	Protein design	Soluble protein?	Processed protein?	Is the homotrimer detected in WB?
6168 Strep II-iKflB	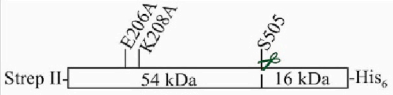	yes	yes	no
6223 Strep II-ALFA-iKflB	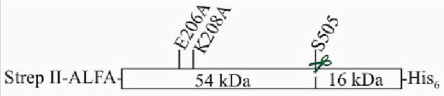	yes	yes	no
6224 Strep II-iKflB-504-ALFA	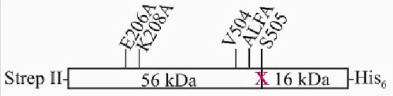	no	no	no
6336 Strep II-ALFA-GS24-iKflB		yes	yes	no
6338 Strep II-eGFP-GS24-KflB	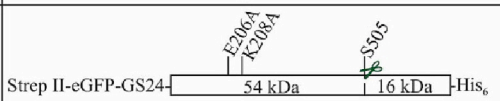	yes	yes	yes

B

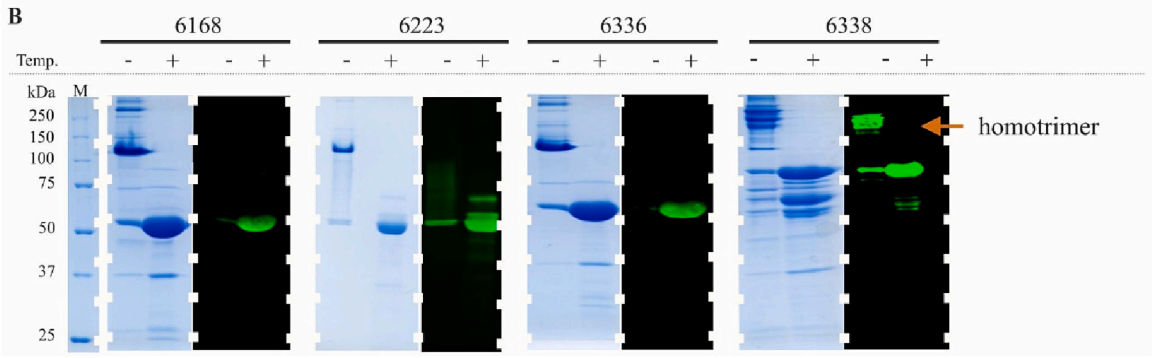

Fig. 9. Engineering an iKflB construct for the detection of heparosan. (A) Overview of the designed constructs. Green scissors indicate that the constructs show the expected molecular weight after CTD cleavage. Construct 6224 was insoluble and appeared to have a non-processed CTD (magenta x).
(B) SDS-PAGE of purified 6168, 6223, 6336, and 6338 and corresponding Western Blot analysis. Strep-tag II (green channel), M – marker, T – temperature, "+" – denatured samples. (For interpretation of the references to colour in this figure legend, the reader is referred to the web version of this article.)

However, K_D values of 10^{-4} to 10^{-6} M for low affinity GAG binders have been reported as well (Xu et al., 2022). Previous studies suggested that the engagement of several binding sites (e.g. as a result of separate binding sites in one TSP monomer, as a result of oligomerization, or mediated by the presence of several TSPs in one phage particle) is important to effectively "trap" the phage in the dense network of polymers present on a bacterial cell surface (Leiman et al., 2007; Schwarzer et al., 2009). We hypothesize that heparosan immobilized on blot membranes, ELISA plates and mammalian cell surfaces better mimics the bacterial cell surface, engages several binding sites and thus better stimulates binding through avidity than heparosan in solution. The concentration of iKflB required to detect heparosan ranges from 1 μg/mL (staining of CHO cells) to 1.7 μg/mL (microscale thermophoresis) and 15–20 μg/mL (ELISA, blots). The former concentration is comparable to the concentration of the monoclonal antibodies used in this study (see 2.12), while the latter is one order of magnitude larger. However, the higher amounts required for ELISA and blot assays are unlikely to negatively impact the use of the detection agent, as iKflB, in contrast to monoclonal antibodies, can be conveniently purified from *E. coli* expression cultures in sufficient amounts.

We demonstrated that KflB can partially digest heparan sulfate, which is structurally similar to heparosan (Chen, Li, et al., 2013; DeAngelis et al., 2013). The majority of heparan sulfate is *N*- or *O*-sulfated, and GlcA is partly epimerized to iduronic acid. The modified domains alternate with less processed domains and non-modified domains that are identical to heparosan (Sarrazin et al., 2011). In agreement with observations made with KflA, we hypothesize that KflB digests heparan sulfate in its non- or less-modified domains (Murphy et al., 2004; O'Leary et al., 2013). Despite this catalytic activity, iKflB was not able to detect commercially available heparan sulfate. While the active site of a carbohydrate active enzyme can be comparatively small, e.g. only accommodating a few residues (Stummeyer et al., 2005), polymer binding sites have been described as being considerably larger, accommodating up to 20 residues (Fiebig et al., 2018; Forsee et al., 2006; Keys et al., 2014). Taking into account that <20 % of the heparan sulfate used in this study is unsulfated, it is tempting to speculate that one or two consecutive unmodified heparosan repeating units can be cleaved by the active site of KflB, while the affinity of an extended binding site to e.g. a highly modified heparan sulfate decamer is disrupted and thus not high enough to mediate sufficient binding in the herein employed assay.

Interestingly, iKflB could be used to detect polymer on CHO wt cells,

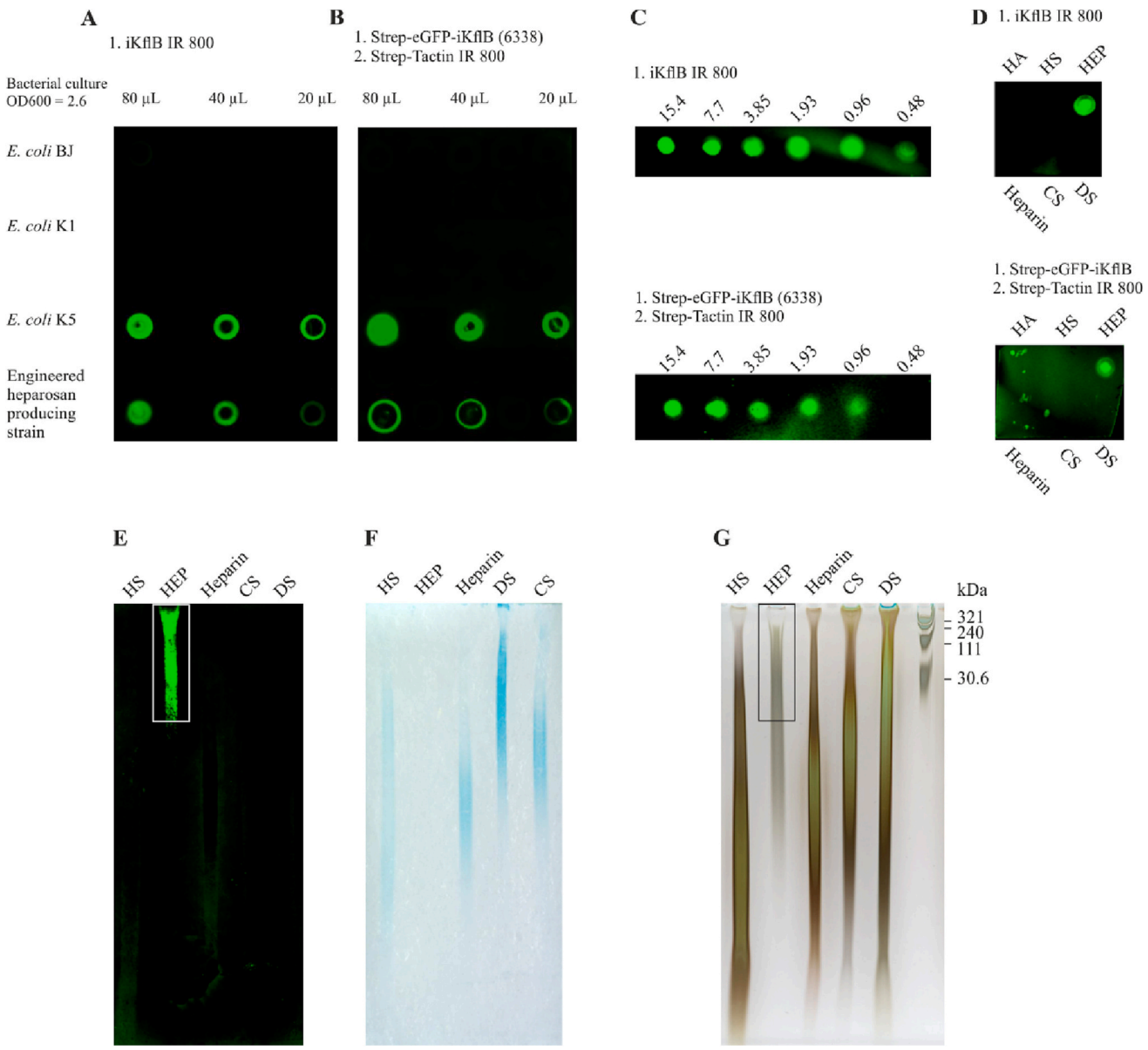

Fig. 10. KflB as detection agent for heparosan immobilized on bacterial surfaces and blot membranes. (A) Direct detection of heparosan using fluorescently labeled iKflB-IR800. (B) Indirect detection using Strep-eGFP-iKflB (6338) followed by fluorescently labeled Strep-Tactin. (C) Determination of the detection limit of heparosan on nitrocellulose membranes using iKflB IR800 (top) and Strep-eGFP-iKflB followed by Strep-Tactin IR800 (bottom). The amounts of unfractionated heparosan spotted in each dot are indicated. (D) The ability to detect hyaluronan (HA), heparan sulfate (HS), heparin, chondroitin sulfate (CS) and dermatan sulfate (DS) was analyzed by dot blot analysis using Strep-eGFP-iKflB (bottom) and iKflB IR 800 (top). Unfractionated heparosan (HEP) was used as positive control. (E) GAGs as indicated were separated by PAGE and subsequently transferred to a positively charged nylon membrane using electro-transfer blotting. Detection of GAGs was achieved using Strep-eGPF-iKflB/Strep-Tactin IR 800 and subsequently using (F) Alcian blue. (G) Corresponding Alcian blue silver stained PAGE for visualization of all GAGs used in the experiment in comparison to Select-HA^{Tm} Lo-Ladder. A box indicates the fraction of heparosan that was detectable using iKflB (compare to white box in (E)). (For interpretation of the references to colour in this figure legend, the reader is referred to the web version of this article.)

while proteoglycan-deficient CHO Δ*XylT2* cells, which lack chondroitin and heparan sulfate (Cuellar et al., 2007), could not be stained using the detection agent. Considering that no GAGs other than heparosan could be detected in any of the herein employed assays, it is reasonable to assume that iKflB detects the less processed or the non-modified domains of heparan sulfate, which seem to be present on (at least) CHO cells. Previous studies have shown both temporal, cell- and tissue-specific variation in modification patterns of heparan sulfate (Attreed et al., 2012; Jenniskens et al., 2000). However, to the best of our knowledge, a commercially available antibody against unmodified heparan sulfate (heparosan) is lacking and the majority (if not all) of the published anti-heparan sulfate antibodies are directed against epitopes present in the processed domains of heparan sulfate (Attreed et al., 2012; Jenniskens et al., 2000; Kurup et al., 2007; Van Den Born et al., 2005). In this study, iKflB had a different and more restricted staining pattern of CHO cells than the sulfation requiring 10E4 antibody. Thus, it is tempting to speculate that iKflB could be a valuable tool to analyze the (sub)cell- and tissue specific heparan sulfate landscape.

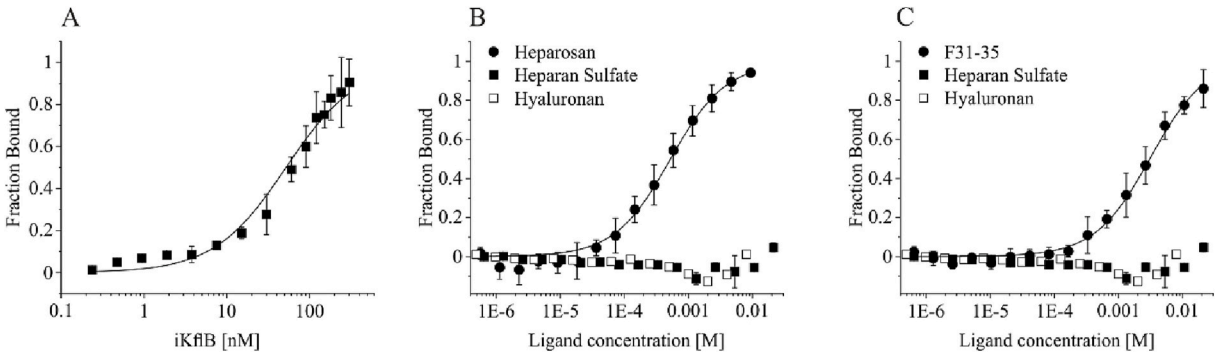

Fig. 11. Analysis of the interaction between iKflB and heparosan using an ELISA-based assay and microscale thermophoresis. (A) The binding of iKflB to surface-bound unfractionated heparosan was analyzed using an ELISA-based assay. The assay was performed as described in Section 2.10 in 3–9 technical replicates. The error bars report standard deviation. (B, C) Microscale thermophoresis using (B) unfractionated heparosan and (C) F31–35 (see Supplementary Fig. 6B) as ligands. Normalized thermophoresis fluorescence averaged from 3 to 4 experiments is plotted against ligand concentration and hyperbolic fits to the data were used to calculate K_D values. The error bars report standard deviation. Heparan sulfate and hyaluronan were used as negative control.

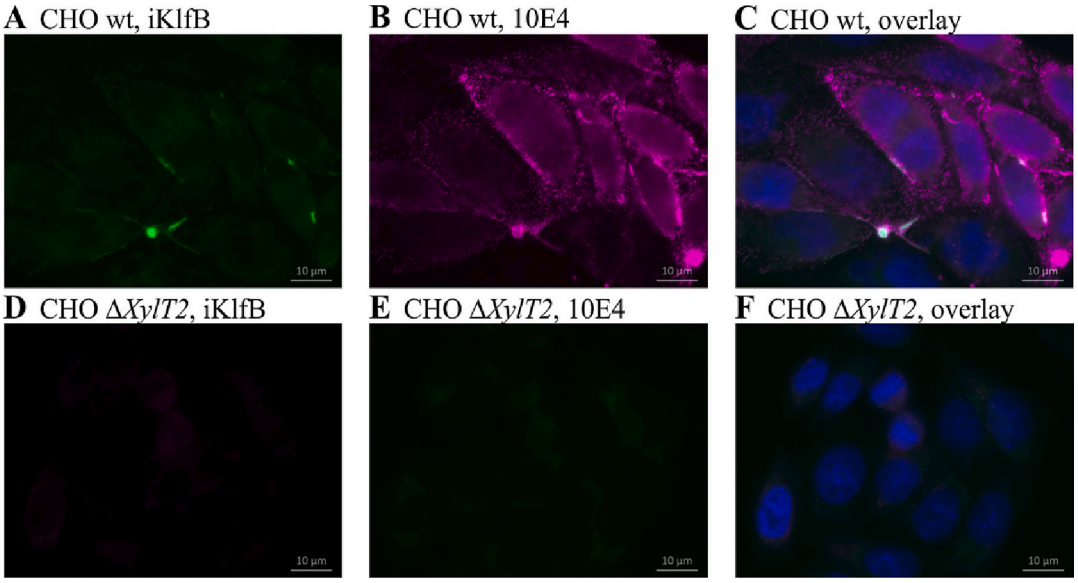

Fig. 12. CHO wt (A, B, C) and proteoglycan-deficient pgsA745 (Δ*XylT2*) (D, E, F) were stained with Strep-eGFP-iKflB (6338, green), and heparan sulfate specific antibody 10E4/Alexa 568 coupled secondary antibody (magenta). Nuclei were stained with Hoechst 33258 (blue, only shown in the overlay C and F). (For interpretation of the references to colour in this figure legend, the reader is referred to the web version of this article.)

Abbreviations

Φ	bacteriophage
Δ	unsaturated uronic acid at the non-reducing end
2AB	2-aminobenzamide
AEC	anion-exchange chromatography
BisTris	Bis-tris methane
CPS	capsular polysaccharide
CTD	C-terminal chaperone domain
DP	degree of polymerization
DTT	dithiothreitol
GAG	glycosaminoglycan
GlcA	glucuronic acid
GlcNAc	*N*-acetylglucosamine
HPLC	high-performance liquid chromatography
IPTG	isopropyl β-D-1-thiogalactopyranoside
KfiA	*N*-acetylglucosaminyltransferase
KfiC	D-glucuronyltransferase
KfiD	UDP-Glc-dehydrogenase
KflA	K5 lyase A
KflB	K5 lyase B
MBP	maltose-binding protein
MS	mass spectrometry
MW	molecular weight
MWCO	molecular weight cut-off
NA	highly sulfated domain of heparan sulfate
NA/NS	intermediately sulfated domain of heparan sulfate
NS	nonsulfated domain of heparan sulfate
OD	optical density
PAGE	polyacrylamide gel electrophoresis
PBS	phosphate-buffered saline
S	serine
SDS	sodium dodecyl sulfate
SEC	Size-Exclusion Chromatography
tetR	tetracycline resistance
TF	trigger factor
TSP	tailspike protein
Tris	tris(hydroxymethyl)aminomethane
Tween® 20	polyethylene glycol sorbitan monolaurate
UDP	uridine diphosphate

UDP-GlcA uridine diphosphate glucuronic acid
UDP-GlcNAc uridine diphosphate *N*-acetylglucosamine
UV ultraviolet
wt wildtype

CrediT authorship contribution statement

M. Mühlenhoff, R. Gerardy-Schahn, B. Priem, T. Fiebig: Conceptualization; F. R. R. Buettner, R. Gerardy-Schahn, B. Priem, T. Fiebig: Funding acquisition; M. Sulewska, M. Berger, M. Damerow, D. Schwarzer, F. F. R. Buettner, M. H. Taft, A. Bethe, H. Bakker: Investigation; M. Sulewska, B. Priem, T. Fiebig, M. H. Taft, H. Bakker: Methodology; M. Mühlenhoff, D. Schwarzer, R. Gerardy-Schahn, B. Priem, T. Fiebig: Supervision; M. Sulewska, M. H. Taft, H. Bakker, T. Fiebig: Visualization; M. Sulewska, T. Fiebig: Roles/Writing - original draft; all authors: Writing - review & editing.

Declaration of competing interest

The authors declare no competing interest.

Data availability

Accession codes for sequences used in this study are provided in the legend of Fig. 1 and in Supplementary Table S2.

Acknowledgements

This study was funded by MHH internal impact orientated funds (LOM) to the Institute of Clinical Biochemistry and by Deutsche Forschungsgemeinschaft (DFG, German Research Foundation) – for Forschungsgruppe FOR2953 (project number 432218849 to F.F.R. Buettner), and project number 412824531 (to T. Fiebig). M. Sulewska and B. Priem acknowledge support from Glyco@Alps (ANR-15-IDEX-OO02). M. Sulewska completed her doctoral thesis in the frame of a French-German graduate program initiated at Université Grenoble Alpes. The study was equally financed by the French and the German partner. We gratefully acknowledge all members of the Institute of Clinical Biochemistry for valuable scientific discussions.

References

Attreed, M., Desbois, M., Van Kuppevelt, T. H., & Bülow, H. E. (2012). Direct visualization of specifically modified extracellular glycans in living animals. *Nature Methods, 9*(5), 477–479. https://doi.org/10.1038/nmeth.1945

Barreteau, H., Richard, E., Drouillard, S., Samain, E., & Priem, B. (2012). Production of intracellular heparosan and derived oligosaccharides by lyase expression in metabolically engineered E. coli K-12. *Carbohydrate Research, 360*, 19–24. https://doi.org/10.1016/j.carres.2012.07.013

Bohlmann, L., Tredwell, G. D., Yu, X., Chang, C. W., Haselhorst, T., Winger, M., … von Itzstein, M. (2015). Functional and structural characterization of a heparanase. *Nature Chemical Biology, 11*(12), 955–957. https://doi.org/10.1038/nchembio.1956

Bond, S. R., & Naus, C. C. (2012). RF-Cloning.org: An online tool for the design of restriction-free cloning projects. *Nucleic Acids Research, 40(Web Server issue), W209-13*. https://doi.org/10.1093/nar/gks396

Boyce, A., & Walsh, G. (2022). Production, characteristics and applications of microbial heparinases. *Biochimie, 198*, 109–140. https://doi.org/10.1016/j.biochi.2022.03.011

Budde, I., Litschko, C., Führing, J. I., Gerardy-Schahn, R., Schubert, M., & Fiebig, T. (2020). An enzyme-based protocol for cell-free synthesis of nature-identical capsular oligosaccharides from Actinobacillus pleuropneumoniae serotype 1. *The Journal of Biological Chemistry, 295*(17), 5771–5784. https://doi.org/10.1074/jbc.RA120.012961

Chavaroche, A. A. E., van den Broek, L. A. M., Boeriu, C., & Eggink, G. (2012). Synthesis of heparosan oligosaccharides by Pasteurella multocida PmHS2 single-action transferases. *Applied Microbiology and Biotechnology, 95*(5), 1199–1210. https://doi.org/10.1007/s00253-011-3813-2

Chen, M., Bridges, A., & Liu, J. (2006). Determination of the substrate specificities of N-acetyl-d-glucosaminyltransferase. *Biochemistry, 45*(40), 12358–12365. https://doi.org/10.1021/bi060844g

Chen, X., Zaro, J. L., & Shen, W. C. (2013). Fusion protein linkers: Property, design and functionality. *Advanced Drug Delivery Reviews, 65*(10), 1357–1369. https://doi.org/10.1016/j.addr.2012.09.039

Chen, Y., Li, Y., Yu, H., Sugiarto, G., Thon, V., Hwang, J., Ding, L., Hie, L., & Chen, X. (2013). Tailored design and synthesis of heparan sulfate oligosaccharide analogues using sequential one-pot multienzyme systems. *Angewandte Chemie - International Edition, 52*(45), 11852–11856. https://doi.org/10.1002/anie.201305667

Cifuente, J. O., Schulze, J., Bethe, A., Di Domenico, V., Litschko, C., Budde, I., … Fiebig, T. (2023). A multi-enzyme machine polymerizes the Haemophilus influenzae type b capsule. *Nature Chemical Biology, 1–13*. https://doi.org/10.1038/s41589-023-01324-3

Clarke, B. R., Esumeh, F., & Roberts, I. S. (2000). Cloning, expression, and purification of the K5 capsular polysaccharide lyase (KflA) from coliphage K5A: Evidence for two distinct K5 lyase enzymes. *Journal of Bacteriology, 182*(13), 3761–3766. https://doi.org/10.1128/JB.182.13.3761-3766.2000

Cress, B. F., Englaender, J. A., He, W., Kasper, D., Linhardt, R. J., & Koffas, M. A. G. (2014). Masquerading microbial pathogens: Capsular polysaccharides mimic host-tissue molecules. *FEMS Microbiology Reviews, 38*(4), 660–697. https://doi.org/10.1111/1574-6976.12056

Cuellar, K., Chuong, H., Hubbell, S. M., & Hinsdale, M. E. (2007). Biosynthesis of chondroitin and heparan sulfate in Chinese Hamster ovary cells depends on xylosyltransferase II. *Journal of Biological Chemistry, 282*(8), 5195–5200. https://doi.org/10.1074/JBC.M611048200

David, G., Bai, X. M., Van Der Schueren, B., Cassiman, J. J., & Van Den Berghe, H. (1992). Developmental changes in heparan sulfate expression: In situ detection with mAbs. *Journal of Cell Biology, 119*(4), 961–975. https://doi.org/10.1083/JCB.119.4.961

DeAngelis, P. L. (2015). Heparosan, a promising 'naturally good' polymeric conjugating vehicle for delivery of injectable therapeutics. *Expert Opinion on Drug Delivery, 12*(3), 349–352. https://doi.org/10.1517/17425247.2015.978282

DeAngelis, P. L., Liu, J., & Linhardt, R. J. (2013). Chemoenzymatic synthesis of glycosaminoglycans: Re-creating, re-modeling and re-designing nature's longest or most complex carbohydrate chains. *Glycobiology, 23*(7), 764–777. https://doi.org/10.1093/glycob/cwt016

DeAngelis, P. L., & White, C. L. (2002). Identification and molecular cloning of a heparosan synthase from Pasteurella multocida type D. *Journal of Biological Chemistry, 277*(9), 7209–7213. https://doi.org/10.1074/jbc.M112130200

DeAngelis, P. L., & White, C. L. (2004). Identification of a distinct, cryptic heparosan synthase from Pasteurella multocida Types A, D, and F. *Journal of Bacteriology, 186*(24), 8529–8532. https://doi.org/10.1128/JB.186.24.8529-8532.2004

Esko, J. D., Stewart, T. E., & Taylor, W. H. (1985). Animal cell mutants defective in glycosaminoglycan biosynthesis. *Proceedings of the National Academy of Sciences, 82*(10), 3197–3201. https://doi.org/10.1073/PNAS.82.10.3197

Fiebig, T., Berti, F., Freiberger, F., Pinto, V., Claus, H., Romano, M. R., … Gerardy-Schahn, R. (2014). Functional expression of the capsule polymerase of Neisseria meningitidis serogroup X: A new perspective for vaccine development. *Glycobiology, 24*(2), 150–158. https://doi.org/10.1093/glycob/cwt102

Fiebig, T., Litschko, C., Freiberger, F., Bethe, A., Berger, M., & Gerardy-Schahn, R. (2018). Efficient solid-phase synthesis of meningococcal capsular oligosaccharides enables simple and fast chemoenzymatic vaccine production. *The Journal of Biological Chemistry, 293*(3), 953–962. https://doi.org/10.1074/jbc.RA117.000488

Forsee, W. T., Cartee, R. T., & Yother, J. (2006). Role of the carbohydrate binding site of the Streptococcus pneumoniae capsular polysaccharide type 3 synthase in the transition from oligosaccharide to polysaccharide synthesis. *The Journal of Biological Chemistry, 281*(10), 6283–6289. https://doi.org/10.1074/jbc.M511124200

France, R. R., Cumpstey, I., Butters, T. D., Fairbanks, A. J., & Wormald, M. R. (2000). Fluorescence labelling of carbohydrates with 2-aminobenzamide (2AB). *Tetrahedron: Asymmetry, 11*(24), 4985–4994. https://doi.org/10.1016/S0957-4166(00)00477-8

Gottschalk, J., Aßmann, M., Kuballa, J., & Elling, L. (2022). Repetitive synthesis of high-molecular-weight hyaluronic acid with immobilized enzyme cascades. *ChemSusChem, 15*(9). https://doi.org/10.1002/cssc.202101071

Götzke, H., Kilisch, M., Martínez-Carranza, M., Sograte-Idrissi, S., Rajavel, A., Schlichthaerle, T., Engels, N., Jungmann, R., Stenmark, P., Opazo, F., & Frey, S. (2019). The ALFA-tag is a highly versatile tool for nanobody-based bioscience applications. *Nature Communications, 10*(1), 1–12. https://doi.org/10.1038/s41467-019-12301-7

Han, Y. H., Garron, M. L., Kim, H. Y., Kim, W. S., Zhang, Z., Ryu, K. S., … Cygler, M. (2009). Structural snapshots of heparin depolymerization by heparin lyase I. *Journal of Biological Chemistry, 284*(49), 34019–34027. https://doi.org/10.1074/JBC.M109.025338

Hänfling, P., Shashkov, A. S., Jann, B., & Jann, K. (1996). Analysis of the enzymatic cleavage (β elimination) of the capsular K5 polysaccharide of Escherichia coli by the K5-specific coliphage: A reexamination. *Journal of Bacteriology, 178*(15), 4747–4750. https://doi.org/10.1128/jb.178.15.4747-4750.1996

He, P., Zhang, X., Xia, K., Green, D. E., Baytas, S., Xu, Y., … DeAngelis, P. L. (2022). Chemoenzymatic synthesis of sulfur-linked sugar polymers as heparanase inhibitors. *Nature Communications 2022 13:1, 13*(1), 1–12. https://doi.org/10.1038/s41467-022-34788-3

Higashi, K., Ly, M., Wang, Z., Masuko, S., Bhaskar, U., Sterner, E., … Linhardt, R. J. (2011). Controlled photochemical depolymerization of K5 heparosan, a bioengineered heparin precursor. *Carbohydrate Polymers, 86*(3), 1365–1370. https://doi.org/10.1016/j.carbpol.2011.06.042

Hodson, N., Griffiths, G., Cook, N., Pourhossein, M., Gottfridson, E., Lind, T., … Roberts, I. S. (2000). Identification that KfiA, a protein essential for the biosynthesis of the Escherichia coli K5 capsular polysaccharide, is an alpha -UDP-GlcNAc glycosyltransferase. The formation of a membrane-associated K5 biosynthetic complex requires KfiA, KfiB, and Kfi. *The Journal of Biological Chemistry, 275*(35), 27311–27315. https://doi.org/10.1074/jbc.M004426200

Jenniskens, G. J., Oosterhof, A., Brandwijk, R., Veerkamp, J. H., & Van Kuppevelt, T. H. (2000). Heparan sulfate heterogeneity in skeletal muscle basal Lamina: demonstration by phage display-derived antibodies. *The Journal of Neuroscience, 20*(11), 4099. https://doi.org/10.1523/JNEUROSCI.20-11-04099.2000

Jing, W., & DeAngelis, P. L. (2004). Synchronized chemoenzymatic synthesis of monodisperse hyaluronan polymers. *The Journal of Biological Chemistry, 279*(40), 42345–42349. https://doi.org/10.1074/jbc.M402744200

Jing, W., Roberts, J. W., Green, D. E., Almond, A., & DeAngelis, P. L. (2017). Synthesis and characterization of heparosan-granulocyte-colony stimulating factor conjugates: A natural sugar-based drug delivery system to treat neutropenia. *Glycobiology, 27*(11), 1052–1061. https://doi.org/10.1093/glycob/cwx072

Keys, T. G., Berger, M., & Gerardy-Schahn, R. (2012). A high-throughput screen for polysialyltransferase activity. *Analytical Biochemistry, 427*(1), 60–68. https://doi.org/10.1016/j.ab.2012.04.033

Keys, T. G., Fuchs, H. L. S., Ehrit, J., Alves, J., Freiberger, F., & Gerardy-Schahn, R. (2014). Engineering the product profile of a polysialyltransferase. *Nature Chemical Biology, 10*(6), 437–442. https://doi.org/10.1038/nchembio.1501

Kiermaier, E., Moussion, C., Veldkamp, C. T., Gerardy-Schahn, R., de Vries, I., Williams, L. G., … Sixt, M. (2016). Polysialylation controls dendritic cell trafficking by regulating chemokine recognition. *Science (New York, N.Y.), 351*(6269), 186–190. https://doi.org/10.1126/science.aad0512

Kizer, M., Li, P., Cress, B. F., Lin, L., Jing, T. T., Zhang, X., … Wang, X. (2018). RNA aptamers with specificity for heparosan and chondroitin glycosaminoglycans. *ACS Omega, 3*(10), 13667–13675. https://doi.org/10.1021/acsomega.8b01853

Kovach, M. E., Elzer, P. H., Steven Hill, D., Robertson, G. T., Farris, M. A., Roop, R. M., & Peterson, K. M. (1995). Four new derivatives of the broad-host-range cloning vector pBBR1MCS, carrying different antibiotic-resistance cassettes. *Gene, 166*(1), 175–176. https://doi.org/10.1016/0378-1119(95)00584-1

Kurup, S., Wijnhoven, T. J. M., Jenniskens, G. J., Kimata, K., Habuchi, H., Li, J. P., … Spillmann, D. (2007). Characterization of anti-heparan sulfate phage display antibodies AO4B08 and HS4E4. *Journal of Biological Chemistry, 282*(29), 21032–21042. https://doi.org/10.1074/JBC.M702073200

Lane, R. S., Haller, F. M., Chavaroche, A. A. E., Almond, A., & DeAngelis, P. L. (2017). Heparosan-coated liposomes for drug delivery. *Glycobiology, 27*(11), 1062–1074. https://doi.org/10.1093/glycob/cwx070

Legoux, R., Lelong, P., Jourde, C., Feuillerat, C., Capdevielle, J., Sure, V., Ferran, E., Kaghad, M., Delpech, B., Shire, D., Ferrara, P., Loison, G., & Salomé, M. (1996). N-acetyl-heparosan lyase of Escherichia coli K5: Gene cloning and expression. *Journal of Bacteriology, 178*(24), 7260–7264. https://doi.org/10.1128/jb.178.24.7260-7264.1996

Leiman, P. G., Battisti, A. J., Bowman, V. D., Stummeyer, K., Mühlenhoff, M., Gerardy-Schahn, R., … Molineux, I. J. (2007). The structures of bacteriophages K1E and K1-5 explain processive degradation of polysaccharide capsules and evolution of new host specificities. *Journal of Molecular Biology, 371*(3), 836–849. https://doi.org/10.1016/j.jmb.2007.05.083

Leroux, M., & Priem, B. (2016). Chaperone-assisted expression of KfiC glucuronyltransferase from Escherichia coli K5 leads to heparosan production in Escherichia coli BL21 in absence of the stabilisator KfiB. *Applied Microbiology and Biotechnology*. https://doi.org/10.1007/s00253-016-7745-8

Litschko, C., Budde, I., Berger, M., & Fiebig, T. (2021). Exploitation of capsule polymerases for enzymatic synthesis of polysaccharide antigens used in glycoconjugate vaccines. *Methods in Molecular Biology (Clifton, N.J.), 2183*, 313–330. https://doi.org/10.1007/978-1-0716-0795-4_16

Liu, H., & Naismith, J. H. (2008). An efficient one-step site-directed deletion, insertion, single and multiple-site plasmid mutagenesis protocol. *BMC Biotechnology, 8*(1), 91. https://doi.org/10.1186/1472-6750-8-91

Ludwigs, U., Elgavish, A., Esko, J. D., Meezan, E., & Rodén, L. (1987). Reaction of unsaturated uronic acid residues with mercuric salts. Cleavage of the hyaluronic acid disaccharide 2-acetamido-2-deoxy-3-O-(beta-D-gluco-4-enepyranosyluronic acid)-D-glucose. *The Biochemical Journal, 245*(3), 795–804. https://doi.org/10.1042/bj2450795

Maloney, F. P., Kuklewicz, J., Corey, R. A., Bi, Y., Ho, R., Mateusiak, L., … Zimmer, J. (2022). Structure, substrate recognition and initiation of hyaluronan synthase. *Nature, 604*(7904), 195–201. https://doi.org/10.1038/s41586-022-04534-2

Merry, C. L. R., Lindahl, U., Couchman, J., & Esko, J. D. (2022). Proteoglycans and sulfated flycosaminoglycans. *Essentials of Glycobiology*. https://doi.org/10.1101/GLYCOBIOLOGY.4E.17

Miller, T., Goude, M. C., Mcdevitt, T. C., & Temenoff, J. S. (2014). Molecular engineering of glycosaminoglycan chemistry for biomolecule delivery. *Acta Biomaterialia, 10*(4), 1705–1719. https://doi.org/10.1016/J.ACTBIO.2013.09.039

Mühlenhoff, M., Stummeyer, K., Grove, M., Sauerborn, M., & Gerardy-Schahn, R. (2003). Proteolytic processing and oligomerization of bacteriophage-derived endosialidases. *Journal of Biological Chemistry, 278*(15), 12634–12644. https://doi.org/10.1074/jbc.M212048200

Murphy, K. J., Merry, C. L. R., Lyon, M., Thompson, J. E., Roberts, I. S., & Gallagher, J. T. (2004). A new model for the domain structure of heparan sulfate based on the novel specificity of K5 lyase. *Journal of Biological Chemistry, 279*(26), 27239–27245. https://doi.org/10.1074/jbc.M401774200

Na, L., Yu, H., McArthur, J. B., Ghosh, T., Asbell, T., & Chen, X. (2020). Engineer P. multocida heparosan synthase 2 (PmHS2) for size-controlled synthesis of longer heparosan oligosaccharides. *ACS Catalysis, 10*(11), 6113–6118. https://doi.org/10.1021/acscatal.0c01231

O'Leary, T. R., Xu, Y., & Liu, J. (2013). Investigation of the substrate specificity of K5 lyase a from K5A bacteriophage. *Glycobiology, 23*(1), 132–141. https://doi.org/10.1093/glycob/cws136

Osawa, T., Sugiura, N., Shimada, H., Hirooka, R., Tsuji, A., Shirakawa, T., Fukuyama, K., Kimura, M., Kimata, K., & Kakuta, Y. (2009). Crystal structure of chondroitin polymerase from Escherichia coli K4. *Biochemical and Biophysical Research Communications, 378*(1), 10–14. https://doi.org/10.1016/j.bbrc.2008.08.121

Otto, N. J., Green, D. E., Masuko, S., Mayer, A., Tanner, M. E., Linhardt, R. J., & DeAngelis, P. L. (2012). Structure/function analysis of Pasteurella multocida heparosan synthases: Toward defining enzyme specificity and engineering novel catalysts. *Journal of Biological Chemistry, 287*(10), 7203–7212. https://doi.org/10.1074/jbc.M111.311704

Peters, H., Jürs, M., Jann, B., Jann, K., Timmis, K. N., & Suermann, D. B. (1985). Monoclonal antibodies to enterobacterial common antigen and to Escherichia coli lipopolysaccharide outer core: Demonstration of an antigenic determinant shared by enterobacterial common antigen and E. coli K5 capsular polysaccharide. *Infection and Immunity, 50*(2), 459–466. https://doi.org/10.1128/iai.50.2.459-466.1985

Peysselon, F., & Ricard-Blum, S. (2014). Heparin–protein interactions: From affinity and kinetics to biological roles. Application to an interaction network regulating angiogenesis. *Matrix Biology, 35*, 73–81. https://doi.org/10.1016/J.MATBIO.2013.11.001

Priem, B., Peroux, J., Colin-Morel, P., Drouillard, S., & Fort, S. (2017). Chemo-bacterial synthesis of conjugatable glycosaminoglycans. *Carbohydrate Polymers, 167*, 123–128. https://doi.org/10.1016/j.carbpol.2017.03.026

Sande, C., & Whitfield, C. (2021). Capsules and extracellular polysaccharides in Escherichia coli and Salmonella. *EcoSal Plus, 9*(2), Article eESP00332020. https://doi.org/10.1128/ecosalplus.ESP-0033-2020

Sarrazin, S., Lamanna, W. C., & Esko, J. D. (2011). Heparan sulfate proteoglycans. *Cold Spring Harbor Perspectives in Biology, 3*(7), Article a004952. https://doi.org/10.1101/CSHPERSPECT.A004952

Scholl, D., Rogers, S., Adhya, S., & Merril, C. R. (2001). Bacteriophage K1-5 encodes two different tail Fiber proteins, allowing it to infect and replicate on both K1 and K5 strains of Escherichia coli. *Journal of Virology, 75*(6), 2509–2515. https://doi.org/10.1128/jvi.75.6.2509-2515.2001

Schulz, E. C., Dickmanns, A., Urlaub, H., Schmitt, A., Mühlenhoff, M., Stummeyer, K., … Ficner, R. (2010). Crystal structure of an intramolecular chaperone mediating triple-B-helix folding. *Nature Structural and Molecular Biology, 17*(2), 210–215. https://doi.org/10.1038/nsmb.1746

Schwarzer, D., Stummeyer, K., Gerardy-Schahn, R., & Mühlenhoff, M. (2007). Characterization of a novel intramolecular chaperone domain conserved in endosialidases and other bacteriophage tail spike and fiber proteins. *Journal of Biological Chemistry, 282*(5), 2821–2831. https://doi.org/10.1074/jbc.M609543200

Schwarzer, D., Stummeyer, K., Haselhorst, T., Freiberger, F., Rode, B., Grove, M., Scheper, T., von Itzstein, M., Mühlenhoff, M., & Gerardy-Schahn, R. (2009). Proteolytic release of the intramolecular chaperone domain confers processivity to endosialidase F. *The Journal of Biological Chemistry, 284*(14), 9465–9474. https://doi.org/10.1074/jbc.M808475200

Sieberth, V., Rigg, G. P., Roberts, I. S., & Jann, K. (1995). Expression and characterization of UDPGlc dehydrogenase (KfiD), which is encoded in the type-specific region 2 of the Escherichia coli K5 capsule genes. *Journal of Bacteriology, 177*(15), 4562–4565. https://doi.org/10.1128/JB.177.15.4562-4565.1995

Sismey-Ragatz, A. E., Green, D. E., Otto, N. J., Rejzek, M., Field, R. A., & DeAngelis, P. L. (2007). Chemoenzymatic synthesis with distinct Pasteurella heparosan synthases: Monodisperse polymers and unnatural structures. *The Journal of Biological Chemistry, 282*(39), 28321–28327. https://doi.org/10.1074/jbc.M701599200

Stummeyer, K., Dickmanns, A., Mühlenhoff, M., Gerardy-Schahn, R., & Ficner, R. (2005). Crystal structure of the polysialic acid-degrading endosialidase of bacteriophage K1F. *Nature Structural & Molecular Biology, 12*(1), 90–96. https://doi.org/10.1038/nsmb874

Sugiura, N., Baba, Y., Kawaguchi, Y., Iwatani, T., Suzuki, K., Kusakabe, T., Yamagishi, K., Kimata, K., Kakuta, Y., & Watanabe, H. (2010). Glucuronyltransferase activity of KfiC from Escherichia coli strain K5 requires association of KfiA: KfiC and KfiA are essential enzymes for production of K5 polysaccharide, N-acetylheparosan. *Journal of Biological Chemistry, 285*(3), 1597–1606. https://doi.org/10.1074/jbc.M109.023002

Thompson, J. E., Pourhossein, M., Waterhouse, A., Hudson, T., Goldrick, M., Derrick, J. P., & Roberts, I. S. (2010). The K5 lyase KflA combines a viral tail spike structure with a bacterial polysaccharide lyase mechanism. *Journal of Biological Chemistry, 285*(31), 23963–23969. https://doi.org/10.1074/jbc.M110.127571

Van Den Born, J., Salmivirta, K., Henttinen, T., Östman, N., Ishimaru, T., Miyaura, S., Yoshida, K., & Salmivirta, M. (2005). Novel heparan sulfate structures revealed by monoclonal antibodies. *Journal of Biological Chemistry, 280*(21), 20516–20523. https://doi.org/10.1074/jbc.M502065200

Volpi, N., & Maccari, F. (2015). Glycosaminoglycan blotting and detection after electrophoresis separation. *Methods in Molecular Biology (Clifton, N.J.), 1312*, 119–127. https://doi.org/10.1007/978-1-4939-2694-7_16

Wienken, C. J., Baaske, P., Rothbauer, U., Braun, D., & Duhr, S. (2010). Protein-binding assays in biological liquids using microscale thermophoresis. *Nature Communications, 1*(1), 1–7. https://doi.org/10.1038/ncomms1093

Willis, L. M., Stupak, J., Richards, M. R., Lowary, T. L., Li, J., & Whitfield, C. (2013). Conserved glycolipid termini in capsular polysaccharides synthesized by ATP-binding cassette transporter-dependent pathways in Gram-negative pathogens. *Proceedings of the National Academy of Sciences of the United States of America, 110*(19), 7868–7873. https://doi.org/10.1073/pnas.1222317110

Xu, D., Prestegard, J. H., Linhardt, R. J., & Esko, J. D. (2022). Proteins that bind sulfated Glycosaminoglycans. In *Essentials of Glycobiology*. Cold Spring Harbor Laboratory Press. https://doi.org/10.1101/glycobiology.4e.38.

Xu, Y., Masuko, S., Takieddin, M., Xu, H., Liu, R., Jing, J., … Liu, J. (2011). Chemoenzymatic synthesis of homogeneous ultralow molecular weight heparins. *Science, 334*(6055), 498–501. https://doi.org/10.1126/SCIENCE.1207478/SUPPL_FILE/XU_SOM.PDF

Yakovlieva, L., & Walvoort, M. T. C. (2020). Processivity in bacterial glycosyltransferases. In *, Vol. 15, Issue 1. ACS chemical biology* (pp. 3–16). American Chemical Society. https://doi.org/10.1021/acschembio.9b00619.

Yan, L., Fu, L., Xia, K., Chen, S., Zhang, F., Dordick, J. S., & Linhardt, R. J. (2020). A revised structure for the glycolipid terminus of Escherichia coli K5 Heparosan capsular polysaccharide. *Biomolecules, 10*(11), 1516. https://doi.org/10.3390/biom10111516

Yuan, H., Tank, M., Alsofyani, A., Shah, N., Talati, N., LoBello, J. C., … Cowman, M. K. (2013). Molecular mass dependence of hyaluronan detection by sandwich ELISA-like assay and membrane blotting using biotinylated hyaluronan binding protein. *Glycobiology, 23*(11), 1270–1280. https://doi.org/10.1093/GLYCOB/CWT064

Zhang, Z., Xie, J., Zhang, F., & Linhardt, R. J (2007). Thin-layer chromatography for the analysis of glycosaminoglycan oligosaccharides. *Anal. Biochem., 371*(1), 118–120. https://doi.org/10.1016/j.ab.2007.07.003

Zhang, C., Liu, L., Teng, L., Chen, J., Liu, J., Li, J., Du, G., & Chen, J. (2012). Metabolic engineering of Escherichia coli BL21 for biosynthesis of heparosan, a bioengineered heparin precursor. *Metabolic Engineering, 14*(5), 521–527. https://doi.org/10.1016/j.ymben.2012.06.005

Zhang, X., Lin, L., Huang, H., & Linhardt, R. J. (2019). Chemoenzymatic synthesis of Glycosaminoglycans. *Accounts of Chemical Research*. https://doi.org/10.1021/ACS.ACCOUNTS.9B00420